



**The Abdus Salam  
International Centre for Theoretical Physics**



**1936-17**

**Advanced School on Synchrotron and Free Electron Laser Sources  
and their Multidisciplinary Applications**

*7 - 25 April 2008*

**X-ray Diffraction  
applied to the study of polycrystalline materials**

P. Scardi  
*University of Trento  
ITALY*

Advanced school on synchrotron and free electron laser sources and their multidisciplinary applications

Trieste 07-25 April, 2008

# X-ray Diffraction

applied to the study of polycrystalline materials

*Prof. Paolo Scardi*

Department of Materials Engineering and  
Industrial Technologies, University of Trento



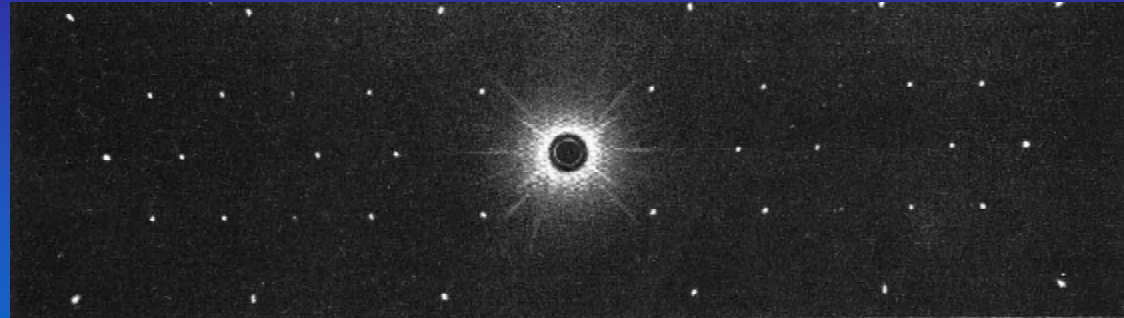
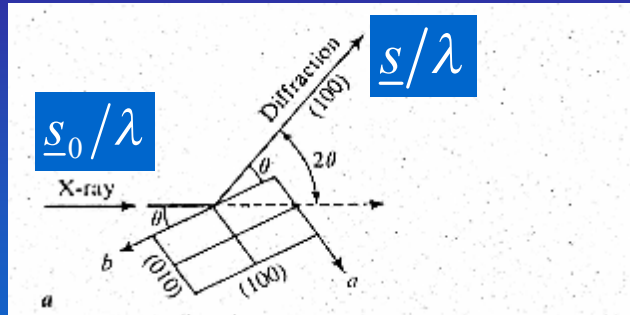


# PRESENTATION OUTLINE

- Basic elements of X-ray diffraction (XRD) theory
- Some advantages and peculiarities of synchrotron radiation XRD (SRXRD)
- SRXRD from nanocrystalline and highly deformed materials



# DIFFRACTION FROM A SINGLE CRYSTAL



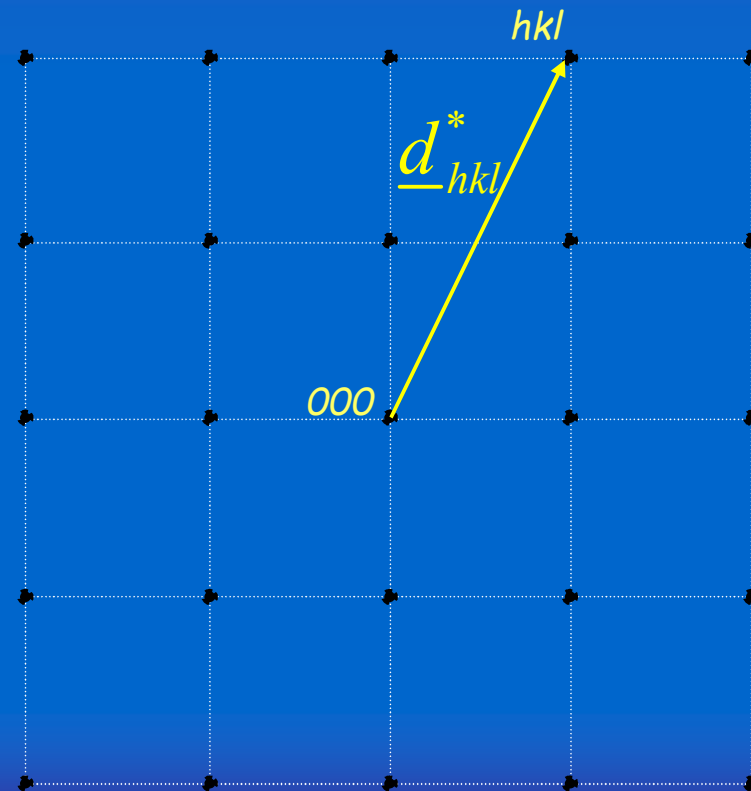
Diffraction conditions correspond to the scattering vector  $(\underline{s} - \underline{s}_0)/\lambda$  being equal to:

$$\frac{\underline{s}}{\lambda} - \frac{\underline{s}_0}{\lambda} = \underline{d}_{hkl}^*$$



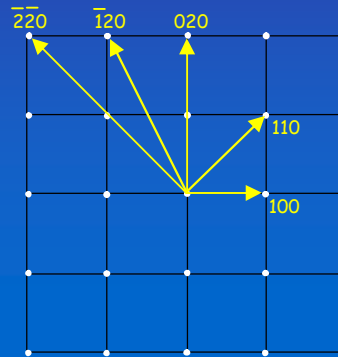
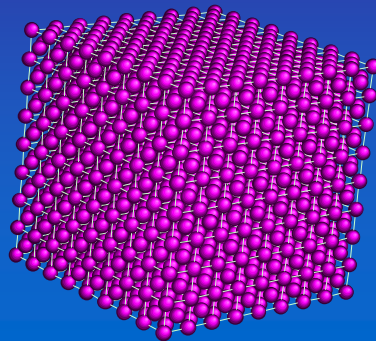
$$\lambda = 2 d_{hkl} \sin \theta$$

Bragg law

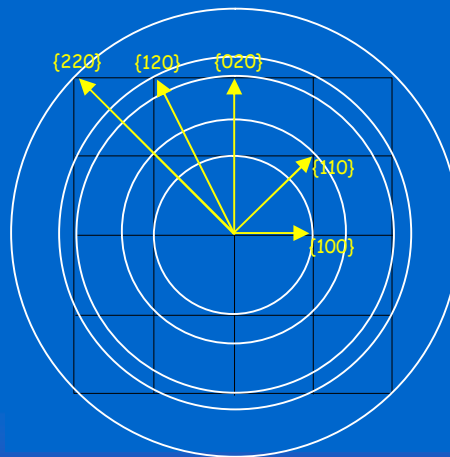
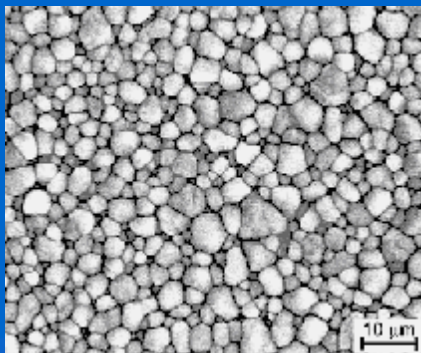




# DIFFRACTION: SINGLE CRYSTAL AND POWDER



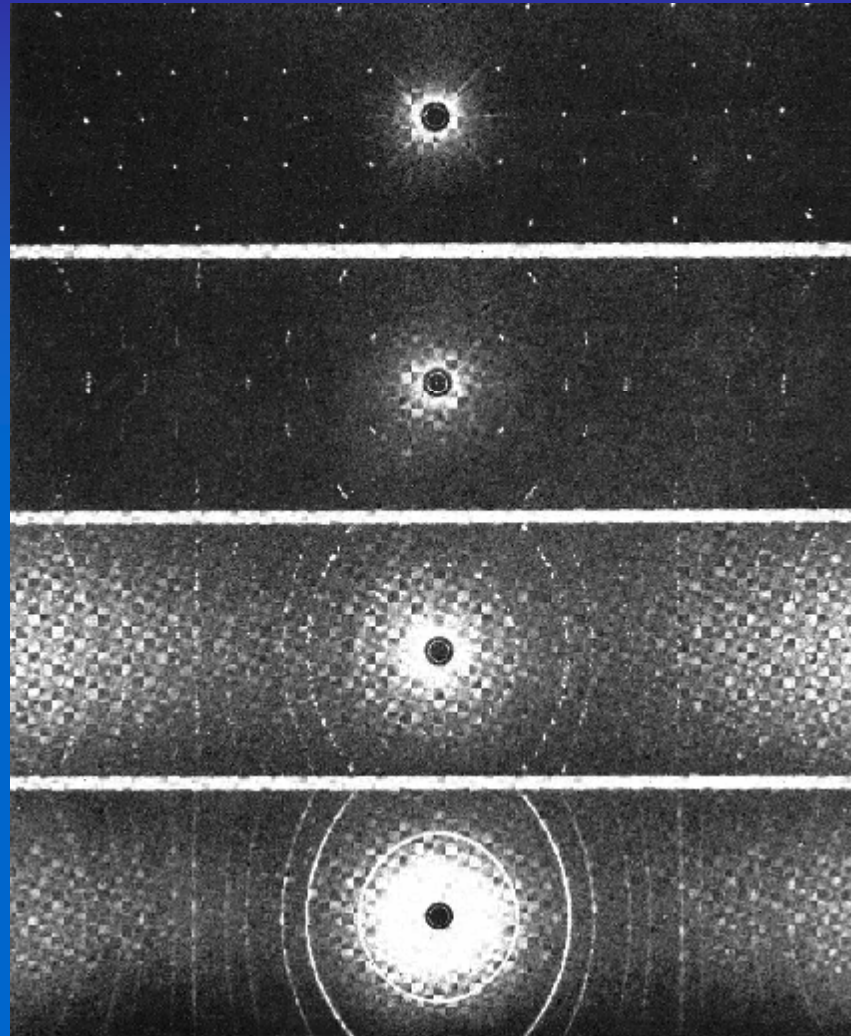
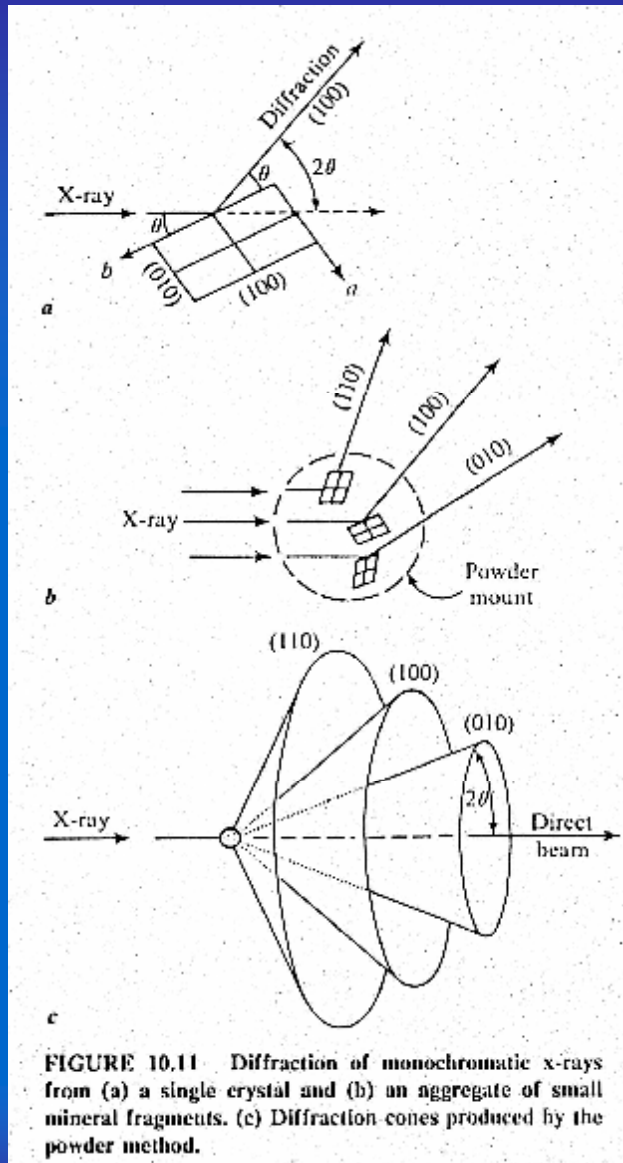
single crystal



powder  
(bulk polycrystalline)



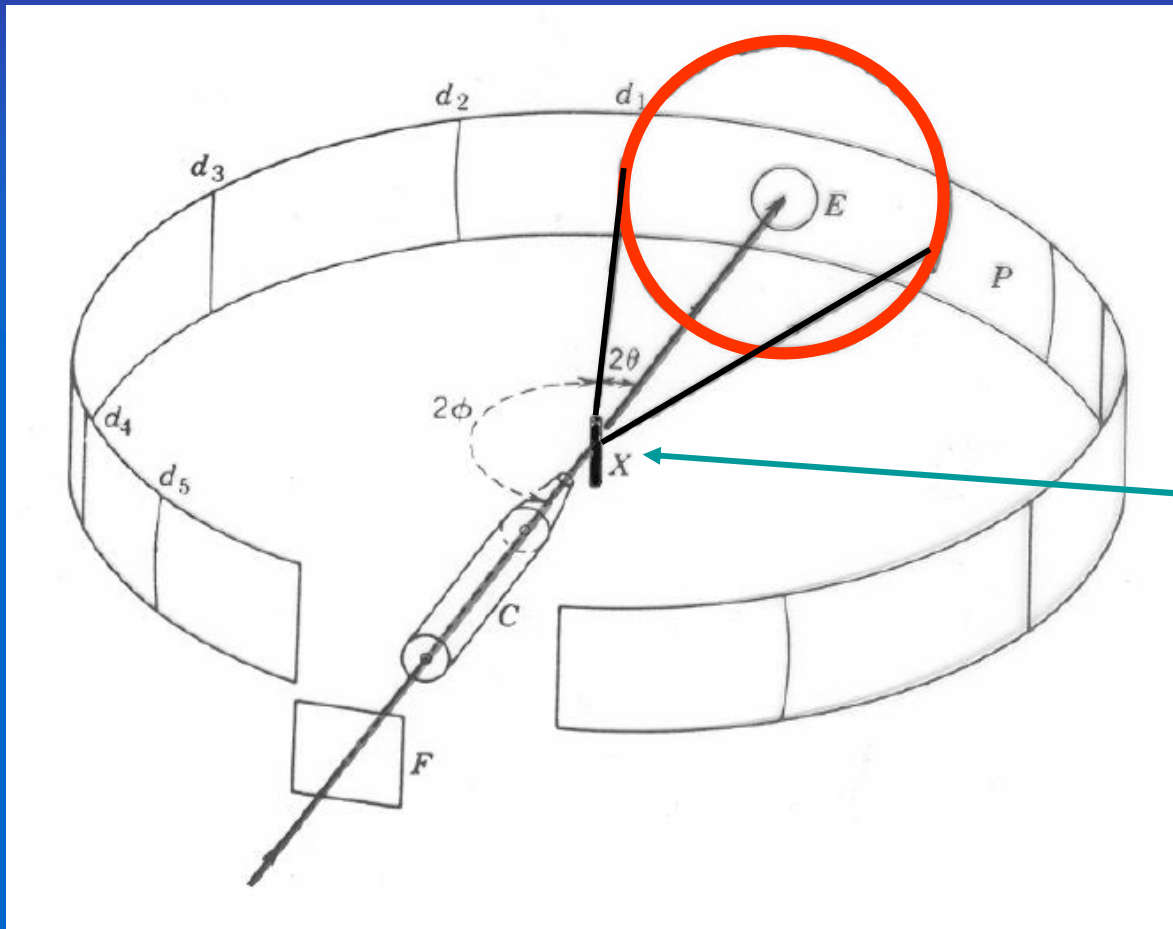
# DIFFRACTION: SINGLE CRYSTAL AND POWDER



(From top to bottom). Fig. 197; Single-crystal rotation photograph of fluorite [100] vertical; Fig. 198; Single crystal rotation photograph of fluorite [200] 2° to vertical; Fig. 199; X-ray photograph of five randomly oriented crystals of fluorite; Fig. 200; Powder photograph of fluorite.



# DEBYE-SCHERRER GEOMETRY



POWDER



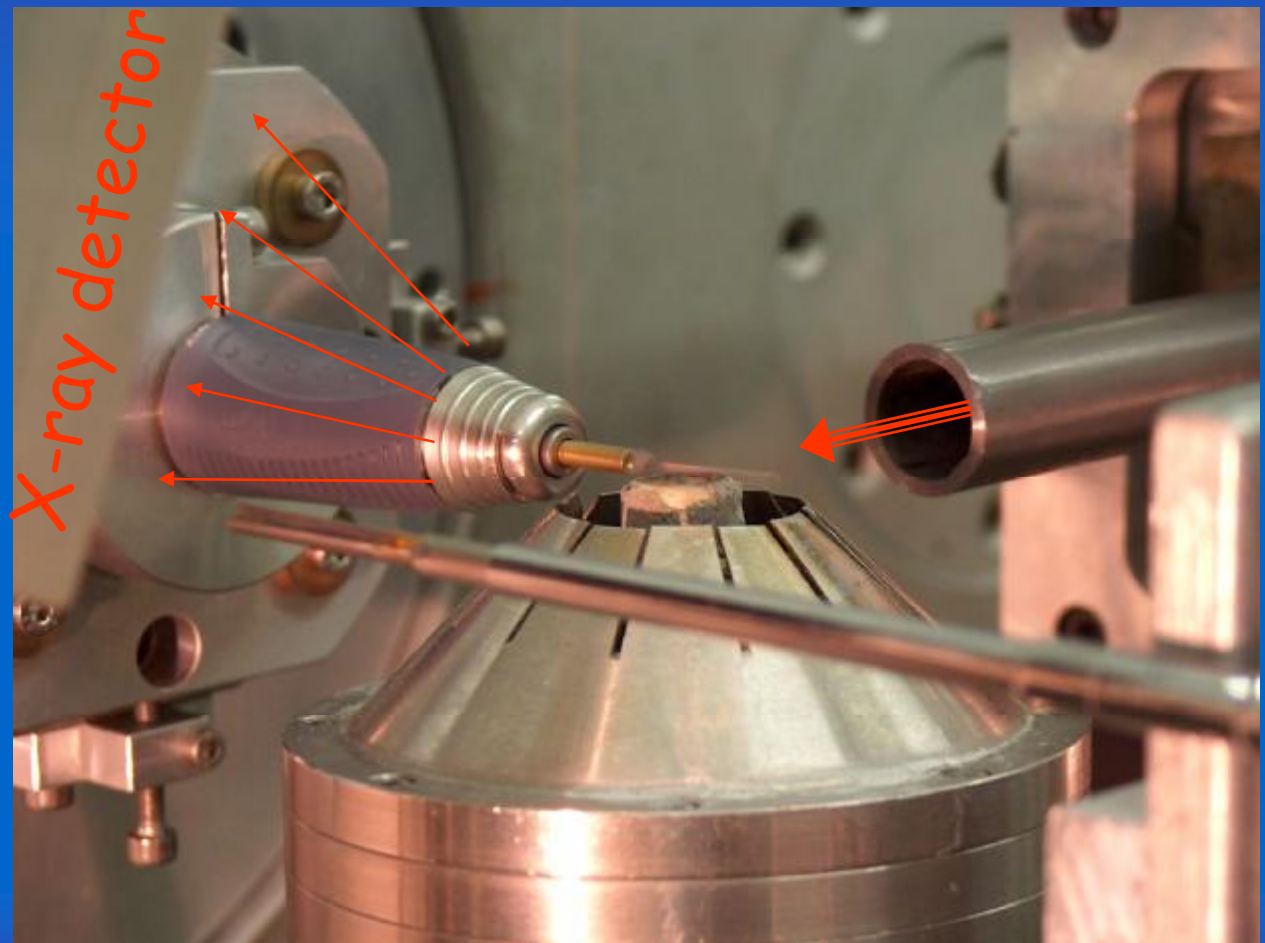
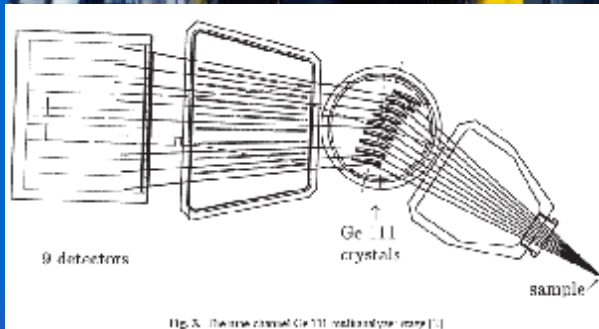
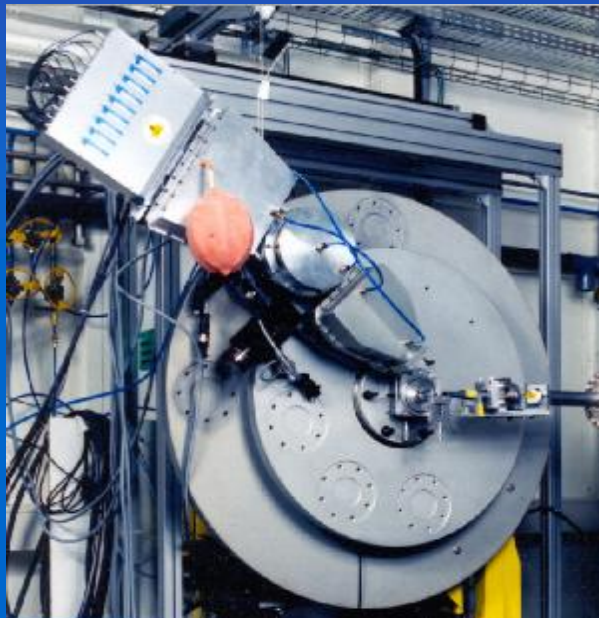


# SRXRD POWDER GEOMETRY: A TYPICAL EXAMPLE

## Parallel beam geometry at ID31 (ESRF)

ID31 Goniometer and  
nine-crystal analyzer

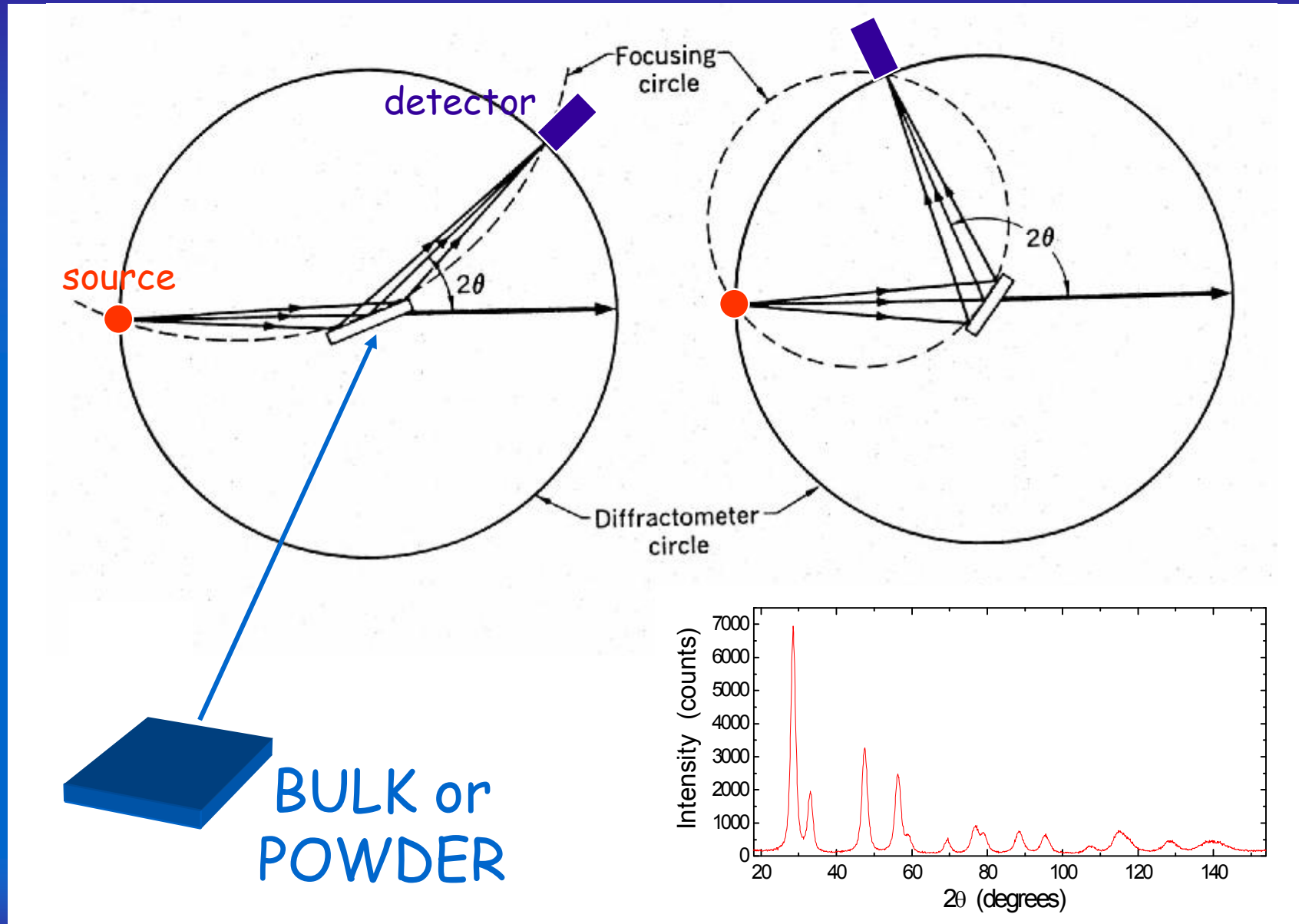
capillary holder / high temperature blower







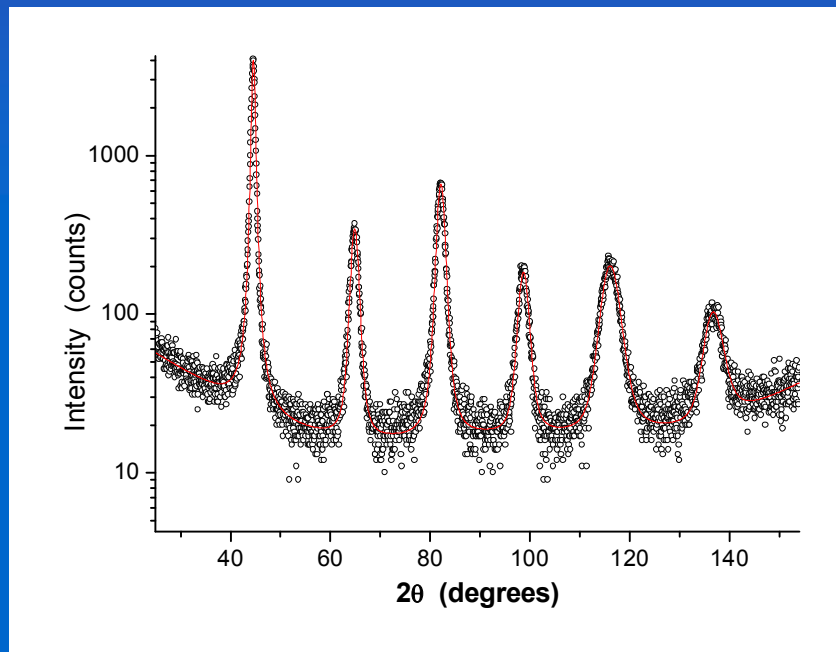
# TYPICAL LAB GEOMETRY: BRAGG-BRENTANO (POWDER)



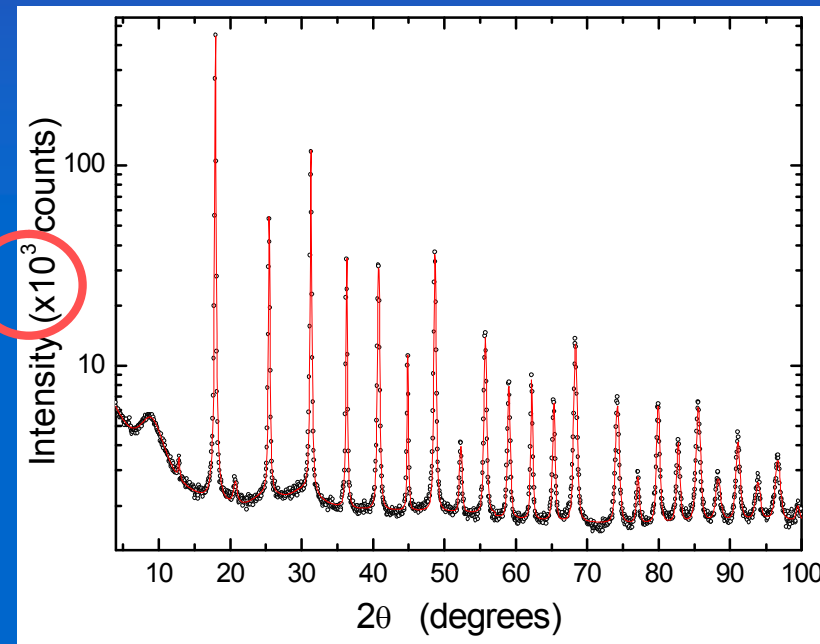


# SOME ADVANTAGES OF SRXRD

1) High brilliance, much better counting statistics / shorter data collection time (→ fast kinetics, in situ studies)



CuK $\alpha$   $\lambda=0.15406$  nm



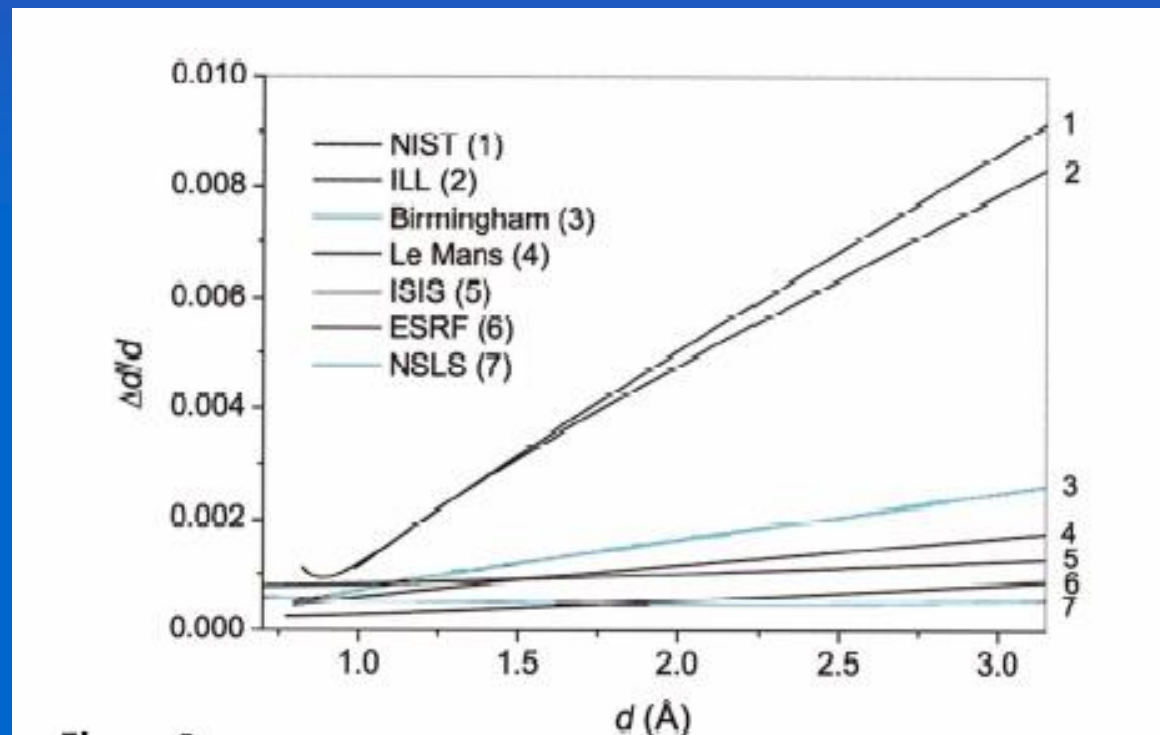
ESRF ID31  $\lambda=0.0632$  nm

M. d'Incau, Leoni & P. Scardi, J. Materials Research 22 (2007) 1744-1753.



# SOME ADVANTAGES OF SRXRD

2) With proper selection of optics, very narrow instrumental profile: increased resolution and accuracy in the measurement of peak position, intensity and profile width/shape.



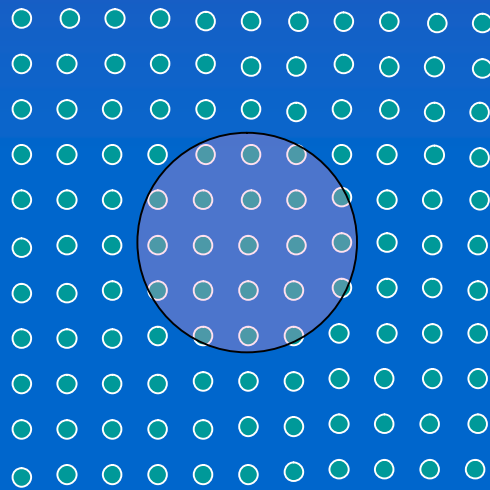
Lab instrument:  
FWHM  $\approx 0.05-0.1^\circ$

ID31 @ESRF:  
FWHM  $\approx 0.003-0.004^\circ$

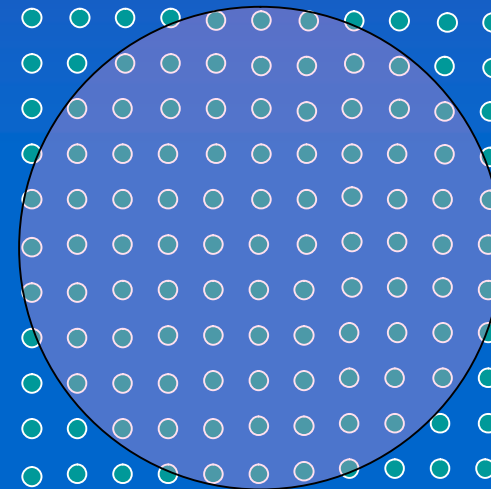


# SOME ADVANTAGES OF SRXRD

3) Extending the accessible region of reciprocal space well beyond what traditional lab instruments can make



$\lambda_1$

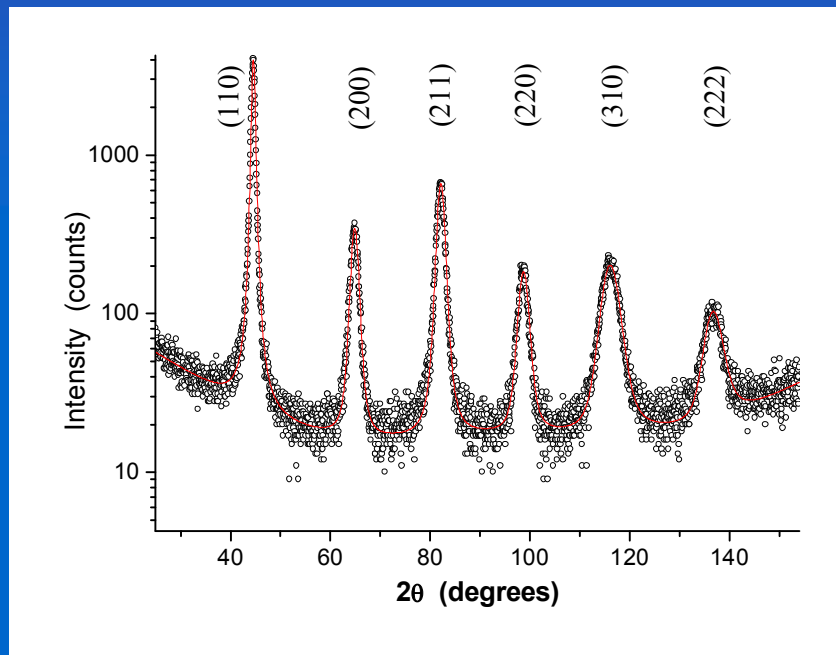


$\lambda_2 < \lambda_1$

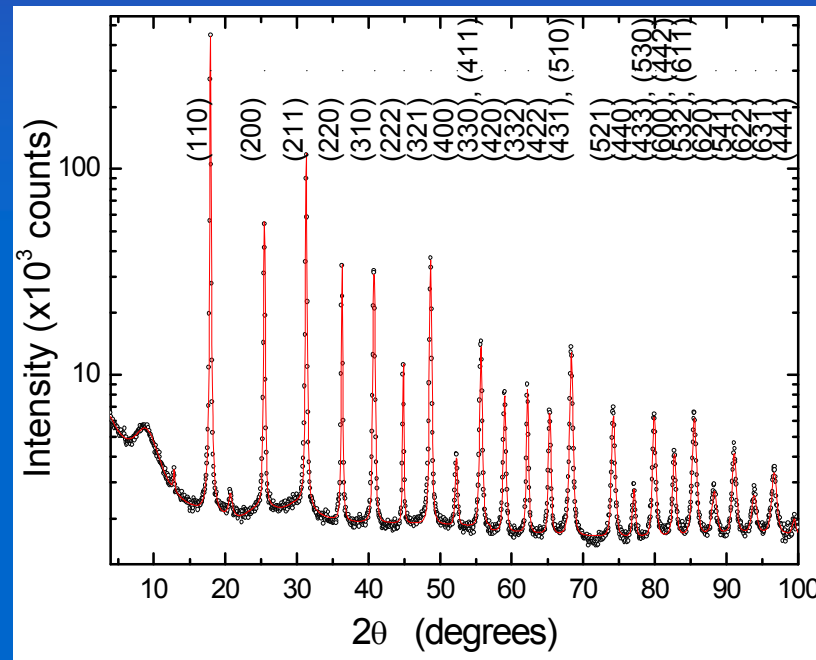


# SOME ADVANTAGES OF SRXRD

3) Extending the accessible region of reciprocal space well beyond what traditional lab instruments can make



CuK $\alpha$   $\lambda=0.15406$  nm



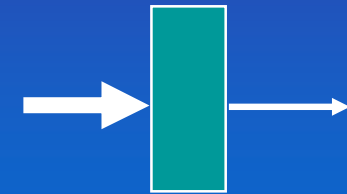
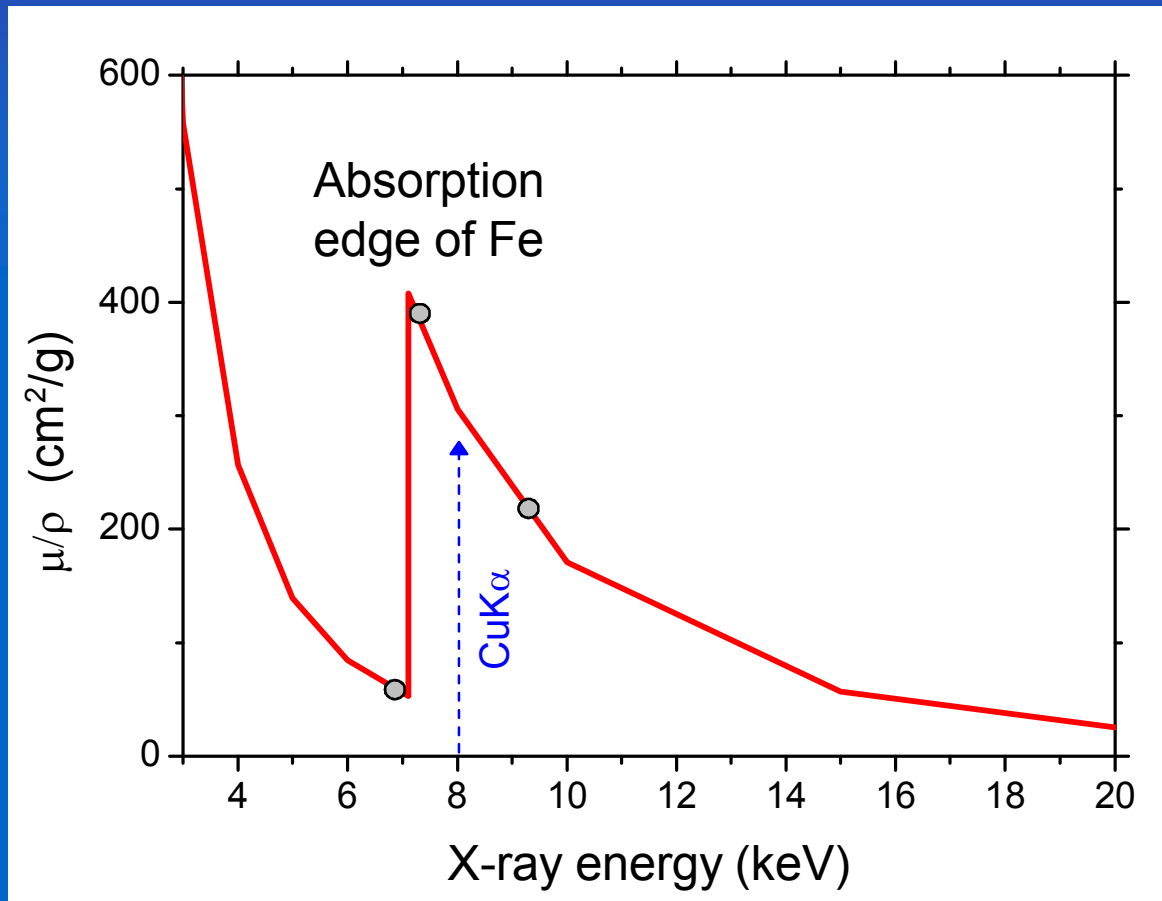
ESRF ID31  $\lambda=0.0632$  nm

M. d'Incau, Leoni & P. Scardi, J. Materials Research 22 (2007) 1744-1753.



# SOME ADVANTAGES OF SRXRD

4) Tuning the energy according to adsorption edges. Resonant scattering, control of fluorescence emission and depth of analysis.



$$I = I_0 e^{-\left(\frac{\mu}{\rho}\right)\rho t}$$



# X-RAY POWDER DIFFRACTION

## Most frequent applications of powder diffraction

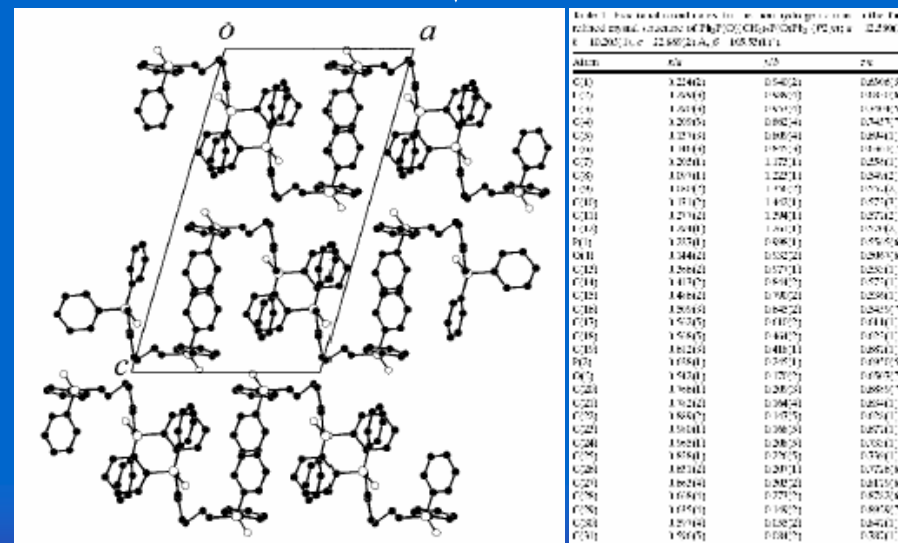
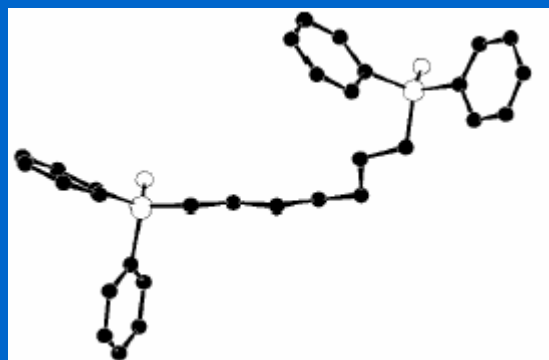
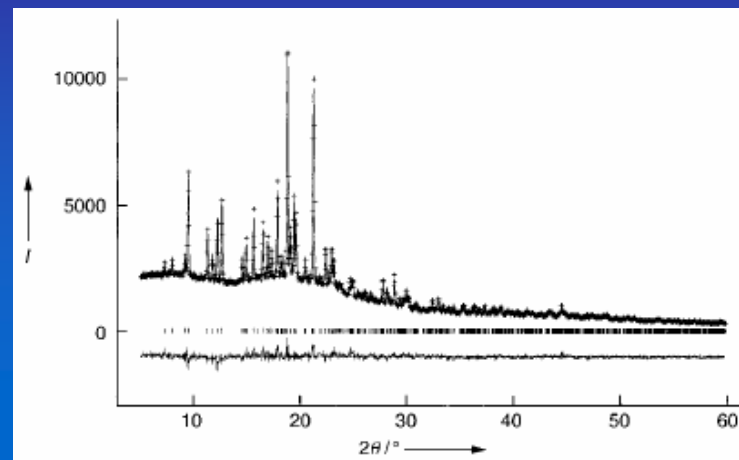
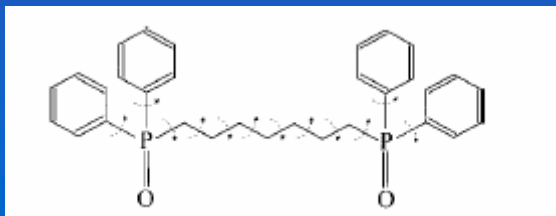
- Crystal structure determination  
(Powder diffraction structure solution and refinement)
- Phase Identification - pure crystalline phases or mixtures  
(Search-Match procedures)
- Quantitative Phase Analysis (QPA)
- Amorphous phase analysis (radial distribution function)
- Crystalline domain size/shape and lattice defect analysis  
(Line Profile Analysis - LPA)
- Determination of preferred orientations (Texture Analysis)
- Determination of residual stress field (Residual Stress Analysis)



# STRUCTURE SOLUTION: WHY POWDER ?

Structure solution of heptamethylene-1,7-bis(diphenylphosphane oxide)

Structural formula  
 $\text{Ph}_2\text{P}(\text{O})(\text{CH}_2)_7\text{P}(\text{O})\text{Ph}_2$



B.M. Kariuki, P. Calcagno, K. D. M. Harris, D. Philp and R.L. Johnston, *Angew. Chem. Int. Ed.* 1999, 38, No. 6, 831-835.

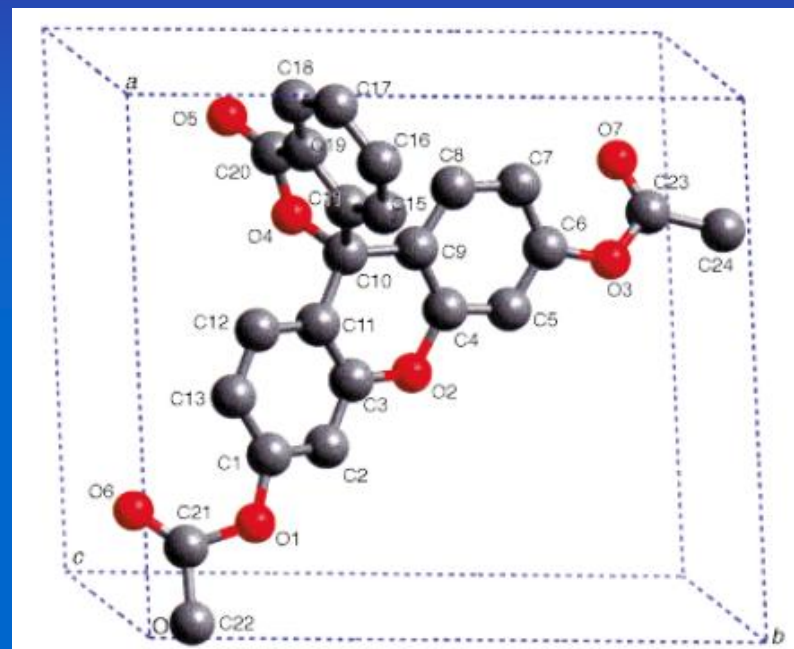
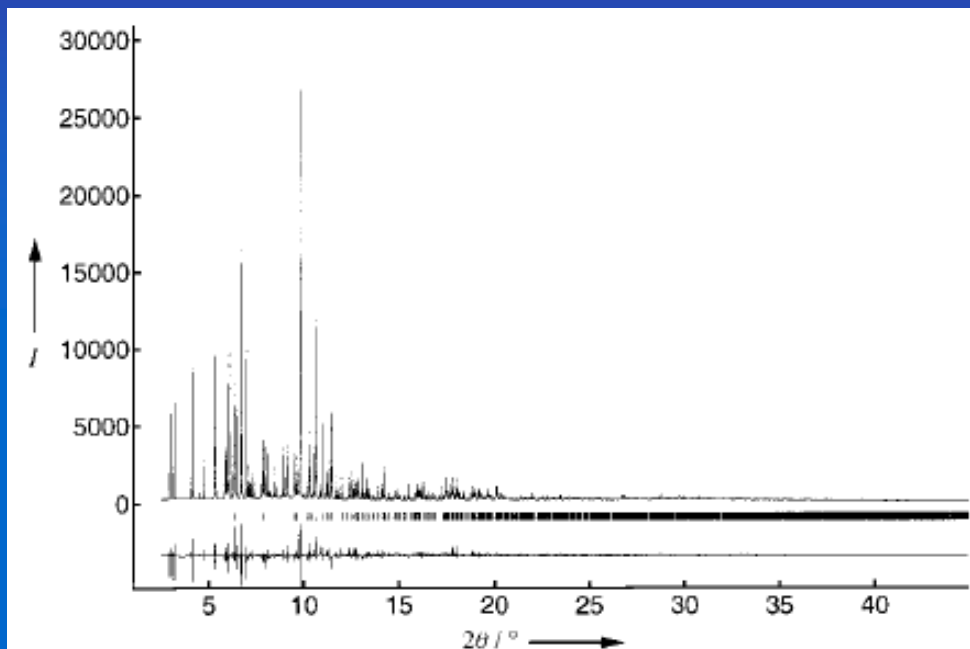




# STRUCTURE SOLUTION & REFINEMENT: SRXRD

Structure solution/refinement of a complex triclinic organic compound ( $C_{24}H_{16}O_7$ )

K. D. Knudsen *et al.*, *Angew. Chem. Int. Ed.*, 37 (1998) 2340



- Narrow peak profiles
- Large number of measurable peaks
- Accurate peak position/intensity
- X-ray energy tuning to adsorption edges



# STRUCTURE SOLUTION & REFINEMENT: SRXRD

Site occupancy in battery electrode material  $\text{LaNi}_{3.55}\text{Mn}_{0.4}\text{Al}_{0.3}\text{Co}_{0.75}$

J.-M. Joubert *et al.*, *J. Appl. Cryst.* 31 (1998) 327

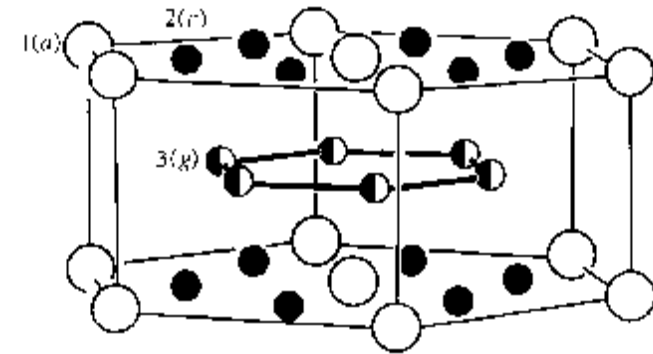
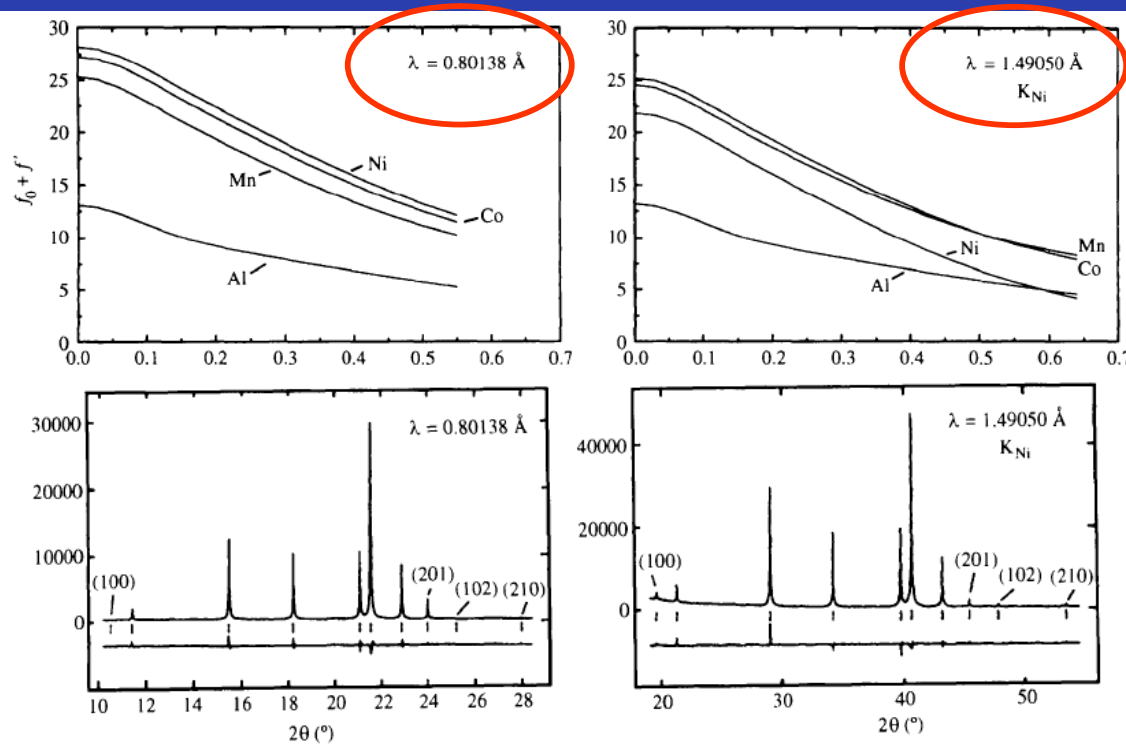


Fig. 1. The crystal structure of  $\text{LaNi}_5$ : the large spheres are La on site 1(a); the small spheres are Ni on sites 2(c) and 3(g)

Atom	Site	x	y	z	B ( $\text{\AA}^2$ )	Occupancy (atoms site <sup>-1</sup> )
La	1(a)	0	0	0	2.06 (2)	1
Ni	2(c)	1/3	2/3	0	2.38 (2)	1.66 (2)
Mn						0.07 (1)
Al						0.032 (4)
Co						0.24 (1)
Ni	3(g)	1/2	0	1/2	1.97 (2)	1.89 (3)
Mn						0.33 (1)
Al						0.267 (6)
Co						0.51 (1)

- Narrow peak profiles
- Large number of measurable peaks
- Accurate peak position/intensity
- X-ray energy tuning to adsorption edges



# STRUCTURE SOLUTION & REFINEMENT: SRXRD

Solving Larger Molecular Crystal Structures from Powder Diffraction Data by Exploiting Anisotropic Thermal Expansion, M. Brunelli et al., *Angew. Chem. Int. Ed.* 42, 2029, (2003)

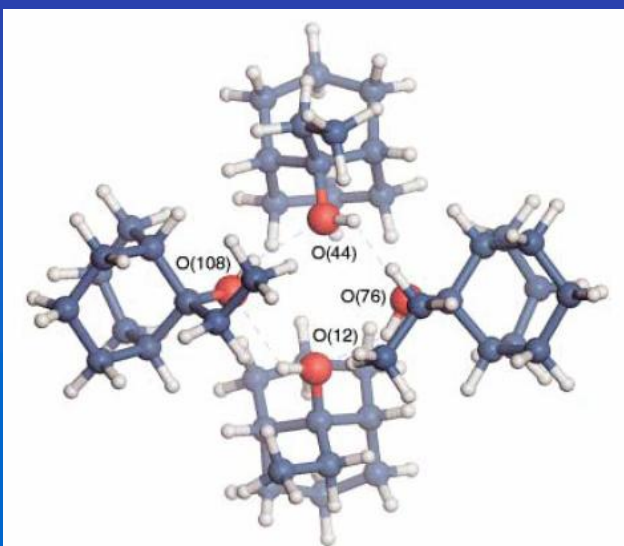
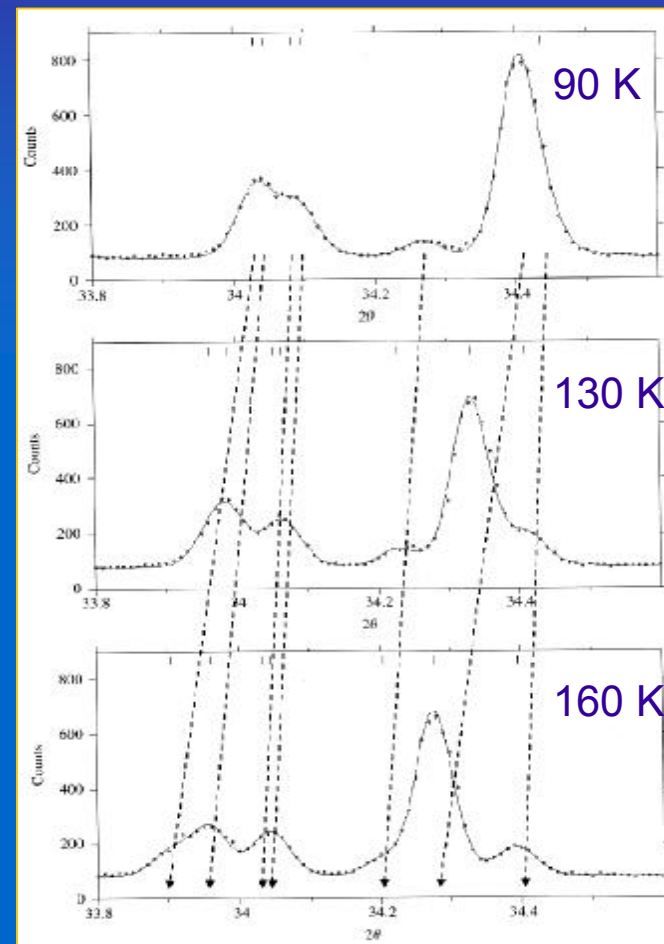


**Figure 3.** View of the arrangement of the four 9-ethylbicyclo[3.3.1]nona-9-ol molecules to form a hydrogen-bonded tetramer. The O—H...O hydrogen bonds are shown with dashed lines: O(12)-O(108) 2.825(4), O(44)-O(76) 2.761(4), O(76)-O(12) 2.804(4), O(108)-O(44) 2.869(4) Å. The crystallographic *c* direction is perpendicular to the plane of the Figure. O red, C blue, H gray.



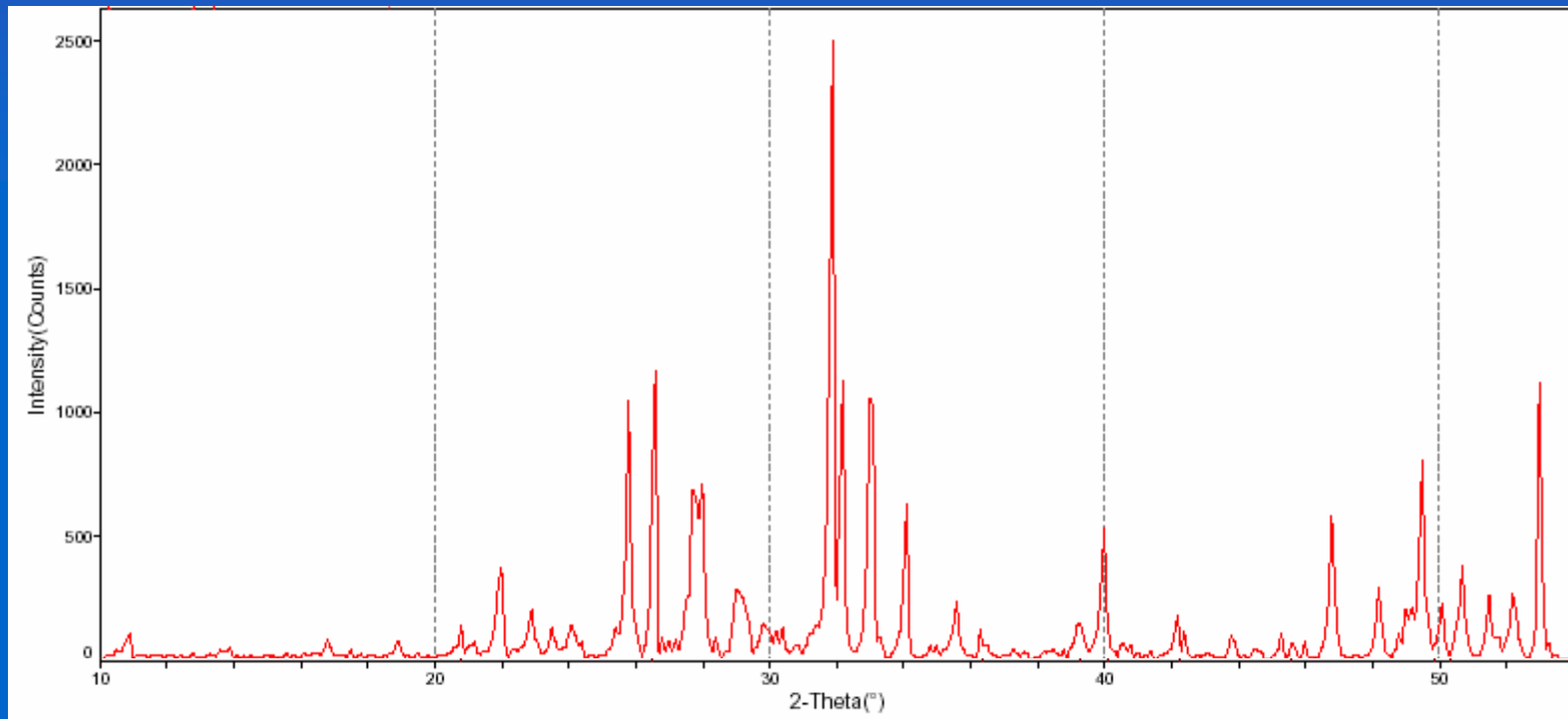
- Narrow peak profiles
- Large number of measurable peaks
- Accurate peak position/intensity
- X-ray energy tuning to adsorption edges
- Anisotropic thermal expansion



# PHASE IDENTIFICATION

Phase identification is one of the first and most diffuse applications of powder diffraction, especially in industry for production, quality control and diagnostics, but also in research.

Each crystalline phase has its own pattern that can be used as a 'fingerprint'



'Fingerprints' of unknown substances can be compared with those of known crystalline phases of a database → *Search-Match procedures*



# PHASE IDENTIFICATION

The most powerful database is the PDF (Powder Diffraction File) by the ICDD (International Centre for Diffraction Data - [www.icdd.com](http://www.icdd.com))



PDF-2  
Peak pos/int



PDF-4  
full structural information

ICDD DDView+ - PDF-4+ 2006 RDB

PDF Card - 04-001-2097

Wavelength: Cu Kα1 1.54056 Å

2θ	d(Å)	I	h	k	l
28.5491	<b>3.124</b>	999	1	1	1
33.0829	2.7055	270	2	0	0
47.4886	<b>1.913</b>	450	2	2	0
56.3453	<b>1.6315</b>	327	3	1	1
59.094	1.562	59	2	2	2
69.4222	1.3527	52	4	0	0
76.7043	1.2414	103	3	3	1
79.0846	1.2099	64	4	2	0
88.4378	1.1045	85	4	2	2
95.4167	1.0413	68	5	1	1
107.2806	0.9565	25	4	4	0
114.7472	0.9146	69	5	3	1
117.3338	0.9018	31	6	0	0

Intensity vs 2θ plot showing peaks at 28.5, 33.1, 47.5, 56.3, 59.1, 69.4, 76.7, 79.1, 88.4, 95.4, 107.3, 114.7, 117.3 degrees.

Atomic Coordinates (2)

Atom	Num	Wyckoff	Symmetry	x	y	z	SOF	ITF	AET
Ce	1	4a	m-3m	0.0	0.0	0.0	1.0	0.7	8-a
O	2	8c	-43m	0.25	0.25	0.25	1.0	1	10-a

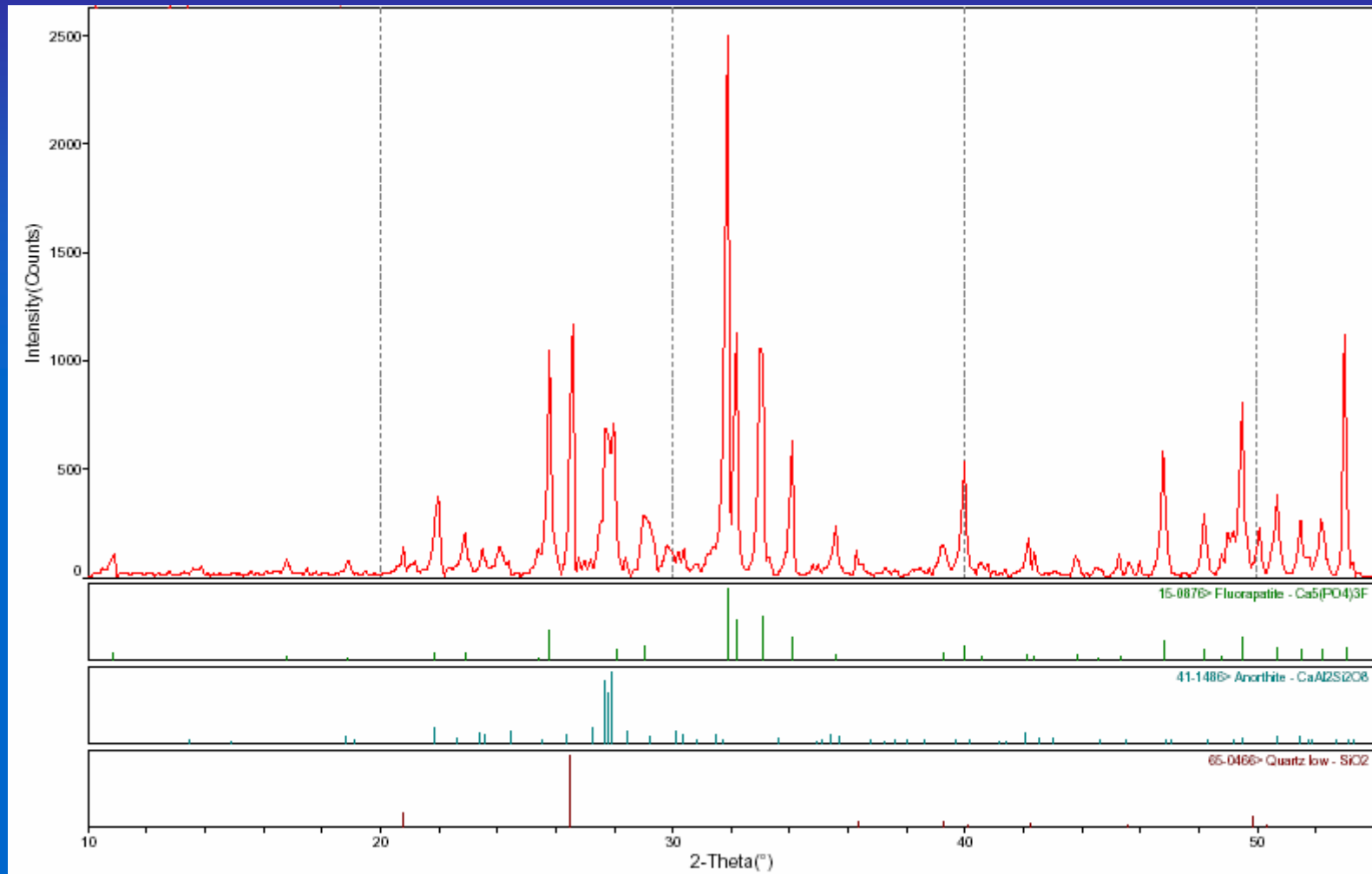
SG Symmetry Operators (48)

Seq	Operator
1	x,y,z
2	-x,-y,-z
3	z,x,y

Crystal structure model showing Ce atoms (white) and O atoms (red) in a cubic lattice.



# PHASE IDENTIFICATION



Automatic search-match procedures are based on peak position / intensity



# THE RIETVELD METHOD

Intensity of the i-th point in the pattern

$$y_{ci} = \sum_j S_j \sum_k I_{k,j} \cdot \phi_{k,j}(2\theta) \cdot P_{k,j} + y_{bi}$$

Diagram illustrating the Rietveld method equation with labels for each term:

- $S_j$ : Scale factor of j-th phase
- $I_{k,j}$ : Integrated Intensity k-th peak of j-th phase
- $\phi_{k,j}(2\theta)$ : Profile function
- $P_{k,j}$ : Preferred Orientation
- $y_{bi}$ : Background term

Using the normalization condition:  $\sum_k x_k = 1$  (not obvious !!)

it is possible to calculate the weight fraction  $x_j$  of the phase  $j$  in a polyphasic mixture as:

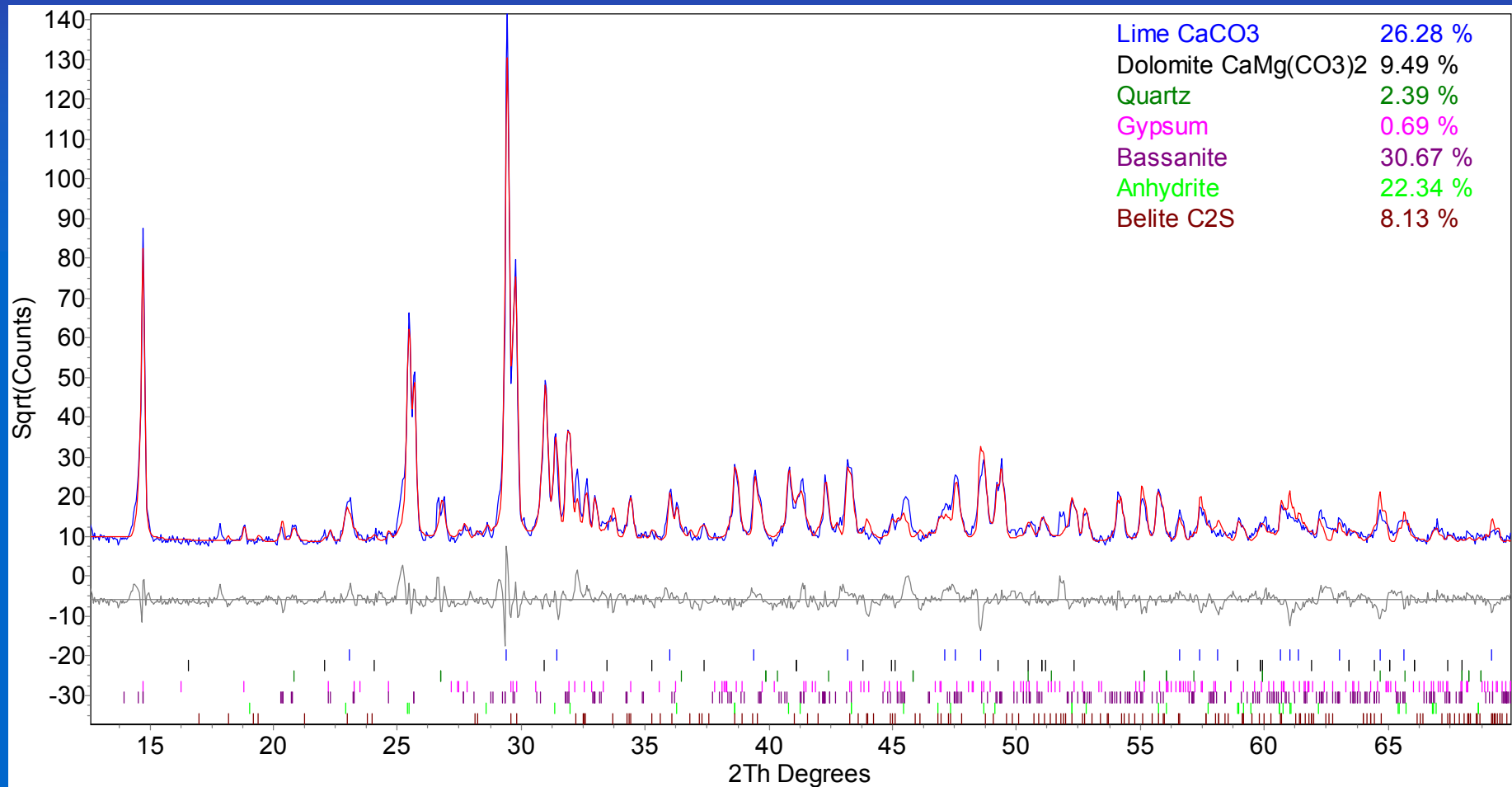
$$x_j = \frac{S_j \rho_j v_j}{\sum_l S_l \rho_l v_l}$$

→ J. Plasier



# RIETVELD-BASED QPA

Example: mixture of mineral phases in a ligand







# STRUCTURE SOLUTION IN MULTIPHASE SAMPLES

Structural and electronic properties of noncubic fullerides  $A'_{40}C_{60}$  ( $A'=Ba,Sr$ )

C.M. Brown *et al.*, Phys. Rev. Let. 83 (1999) 2258

ESRF BM161  $\lambda=0.084884$  nm

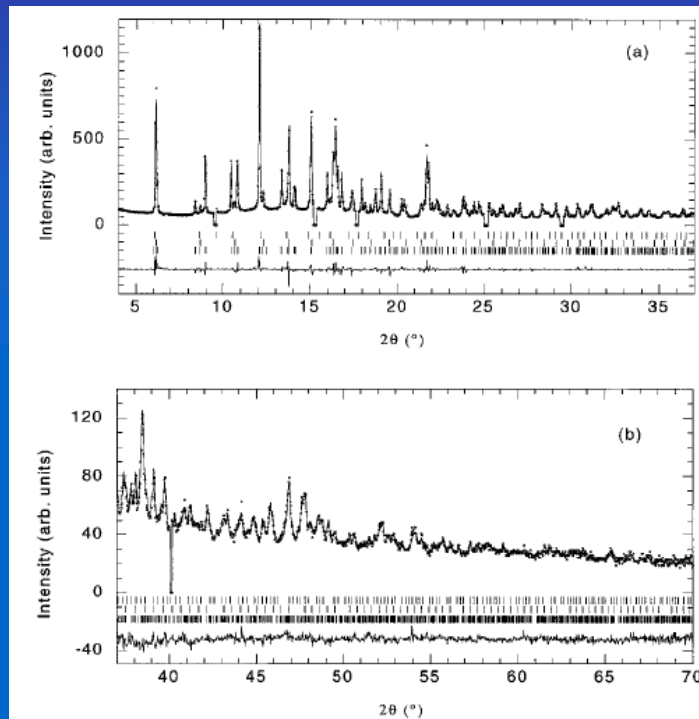


FIG. 2. Final observed (points) and calculated (solid line) synchrotron x-ray powder diffraction profiles for  $Ba_4C_{60}$  at 295 K in the range  $4^\circ$  to  $70^\circ$  ( $\lambda = 0.084884$  Å). The lower panels show the difference profiles and the ticks mark the positions of the Bragg reflections of  $Ba_4C_{60}$  [majority phase: 86.1(2)%, lower most],  $Ba_6C_{60}$  [minority phase: 11.8(1)%, middle], and  $Ba_3C_{60}$  [minority phase: 2.1(1)% upper most]. Some sharp peaks originating from a nonfulleride phase were excluded from the refinement.

- Narrow peak profiles
- Large number of measurable peaks
- Accurate peak position/intensity
- X-ray energy tuning to adsorption edges



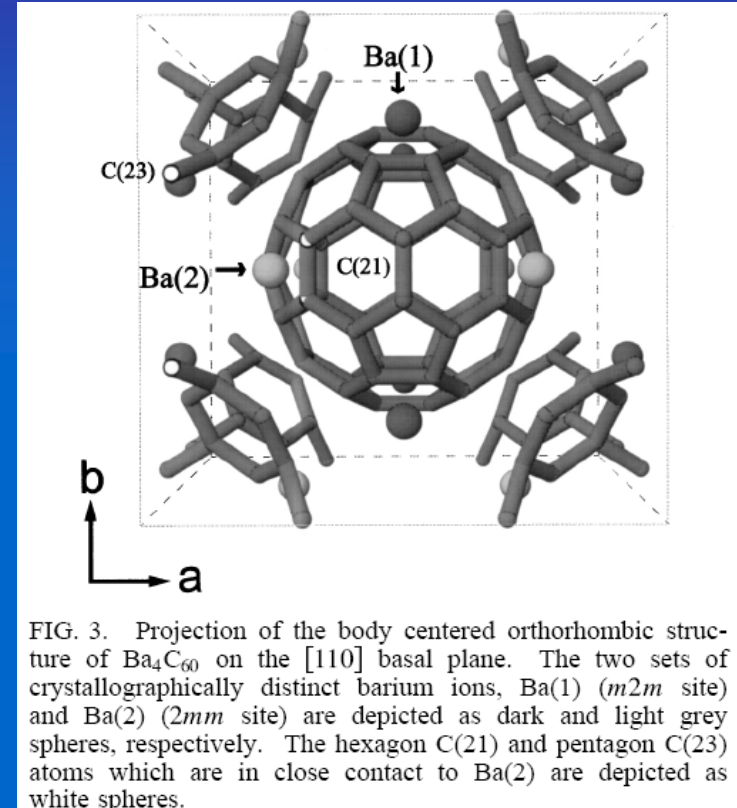
# STRUCTURE SOLUTION IN MULTIPHASE SAMPLES

Structural and electronic properties of noncubic fullerides  $A'_{40}C_{60}$  ( $A'=Ba,Sr$ )

C.M. Brown *et al.*, Phys. Rev. Let. 83 (1999) 2258

TABLE I. Refined parameters for orthorhombic  $Ba_4C_{60}$  obtained from Rietveld refinement of the synchrotron x-ray powder diffraction data at 295 K (space group  $Immm$ ,  $R_{wp} = 5.3\%$ ,  $R_{exp} = 2.6\%$ ). The cell constants are  $a = 11.6101(2)$ ,  $b = 11.2349(2)$ , and  $c = 10.8830(2)$  Å, and the weight fraction of the  $Ba_4C_{60}$  phase is 86.1(2)%. The weight fractions of the minority phases,  $Ba_6C_{60}$  and  $Ba_3C_{60}$  are 11.8(1)% and 2.1(1)%, respectively. The cell constants of cubic  $Ba_6C_{60}$  (space group  $Im\bar{3}$ ) and  $Ba_3C_{60}$  (space group  $Pm\bar{3}n$ ) are 11.1959(2) and 11.338(1) Å, respectively.

Atom	$x/a$	$y/b$	$z/c$	$B_{iso}/\text{Å}^2$ ( $\beta_{11}, \beta_{22}, \beta_{33}$ )
Ba(1)	0.5	0.2034(2)	0.0	1.9(1), 2.9(2), 0.9(1)
Ba(2)	0.2488(1)	0.5	0.0	2.7(1), 3.7(2), 0.6(1)
C(11)	0.3005(2)	0.0	0.0652(1)	0.16(8)
C(12)	0.0	-0.063 88(4)	0.3206(2)	0.16(8)
C(13)	0.10014(6)	-0.127 86(7)	0.2798(2)	0.16(8)
C(21)	0.2003(1)	-0.63 88(4)	0.2389(1)	0.16(8)
C(22)	0.12373(7)	-0.271 0(2)	0.106 82(6)	0.16(8)
C(23)	0.06187(4)	-0.310 5(2)	0.0	0.16(8)
C(31)	0.2240(2)	-0.207 0(1)	0.066 00(3)	0.16(8)
C(32)	0.06187(4)	-0.231 4(1)	0.213 7(1)	0.16(8)
C(33)	0.2622(2)	-0.103 45(6)	0.131 99(8)	0.16(8)



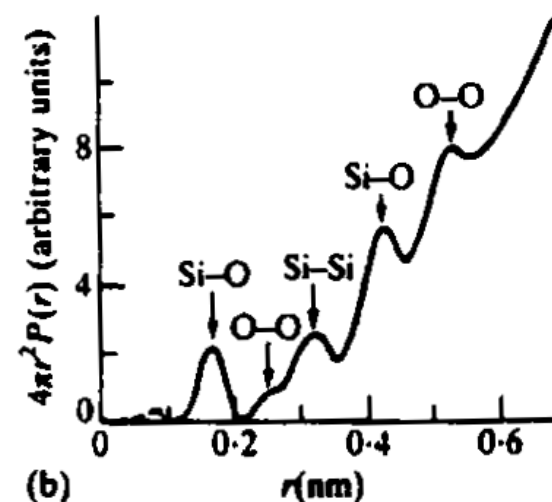
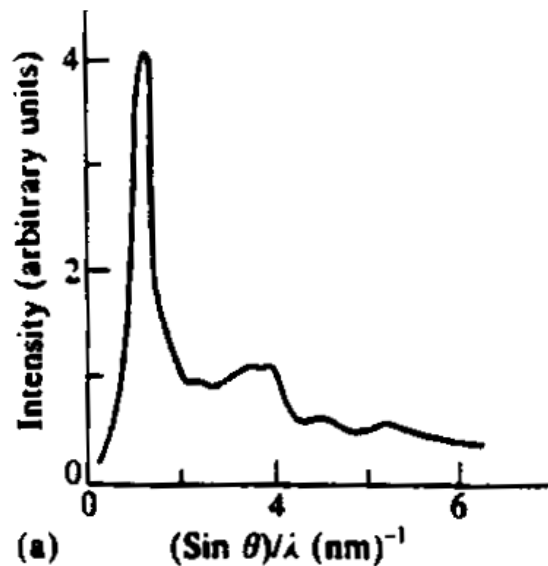
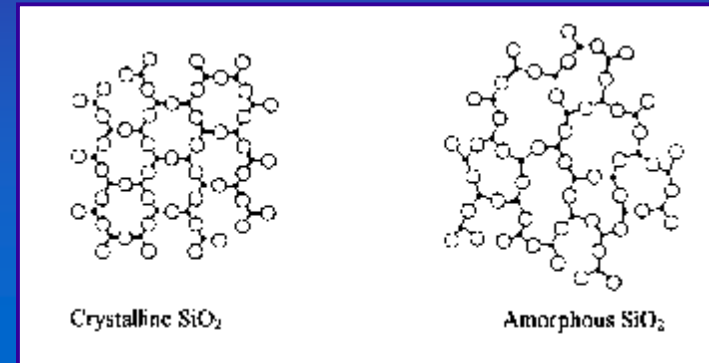
- Narrow peak profiles
- Large number of measurable peaks
- Accurate peak position/intensity
- X-ray energy tuning to adsorption edges



# AMORPHOUS PHASE ANALYSIS

The long-range order typical of crystalline structures is absent in amorphous materials. However, a certain degree of short-range order is always present.

Diffraction can be used to measure the *radial distribution function*, i.e., the probability distribution to find an atom at a distance between  $r$  and  $r+\delta r$  taken from a reference atom.





# PAIR DISTRIBUTION FUNCTION: USE OF SRXRD

Structure of nanocrystalline materials using atomic Pair Distribution Function (PDF) analysis: study of  $\text{LiMoS}_2$ .

V. Petkov *et al.*, *Phys. Rev. B* 65 (2002) 092105

$$PDF : G(r) = 4\pi r [\rho(r) - \rho_0]$$

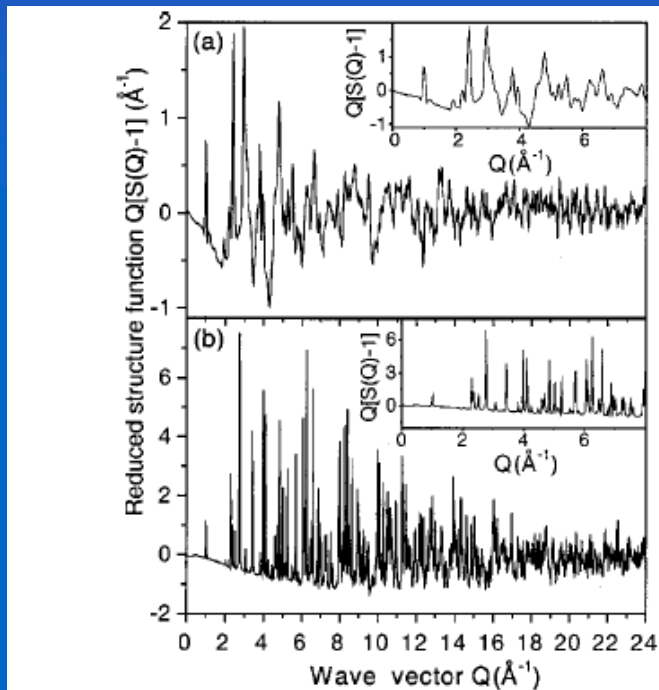


FIG. 1. Experimental structure functions of (a)  $\text{LiMoS}_2$  and (b)  $\text{MoS}_2$ . Note the different scale between (a) and (b). The data are shown in an expanded scale in the insets.

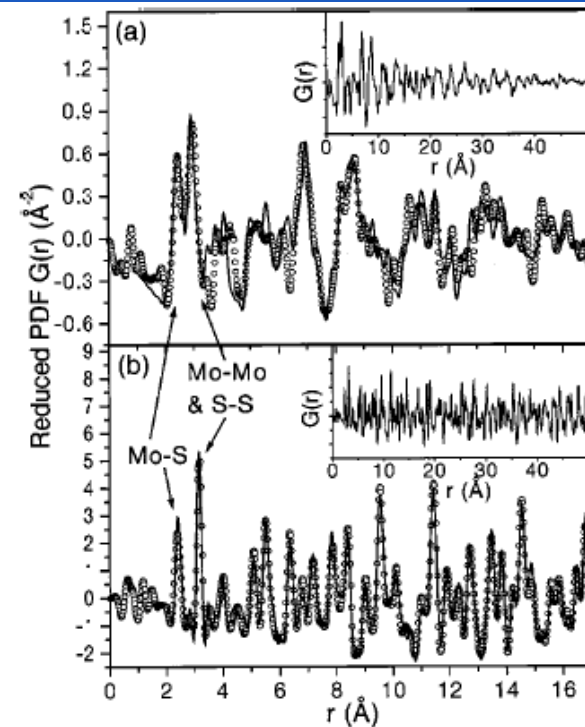


FIG. 2. Experimental (dots) and fitted (solid line) PDF's for  $\text{LiMoS}_2$  (a) and  $\text{MoS}_2$  (b). Note the different scale between (a) and (b). The first two peaks in the PDF's are labeled with the corresponding atomic pairs. The experimental data are shown in an expanded scale in the insets.



# PAIR DISTRIBUTION FUNCTION: USE OF SRXRD

Structure of nanocrystalline materials using atomic Pair Distribution Function (PDF) analysis: study of  $\text{LiMoS}_2$ .

V. Petkov *et al.*, Phys. Rev. B 65 (2002) 092105

$$PDF : G(r) = 4\pi r [\rho(r) - \rho_0]$$

TABLE I. Structural parameters for  $\text{MoS}_2$ . Space group is  $P6_3/mmc$ . Mo is at  $(\frac{1}{3}, \frac{2}{3}, \frac{1}{4})$  and S at  $(\frac{1}{3}, \frac{2}{3}, z)$ .

	PDF	Rietveld	Single crystal <sup>a</sup>
$a$ (Å)	3.169(1)	3.168(1)	3.1604(2)
$c$ (Å)	12.324(1)	12.322(1)	12.295(2)
$z$	0.623(1)	0.625(1)	0.629(1)

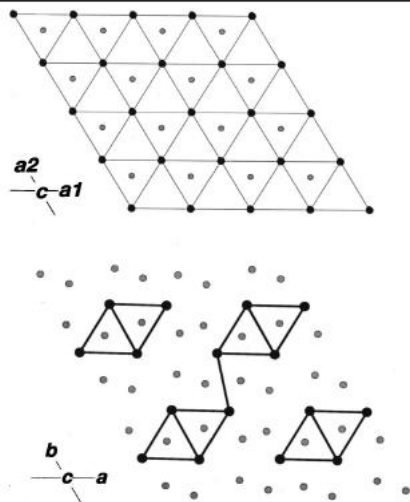


FIG. 4. Projection down the  $c$  axis of the crystal structures of hexagonal  $\text{MoS}_2$  (up) and triclinic  $\text{LiMoS}_2$  (down). The large black circles are Mo atoms and the small gray circles are the S atoms. Li atoms are not shown for the sake of clarity.

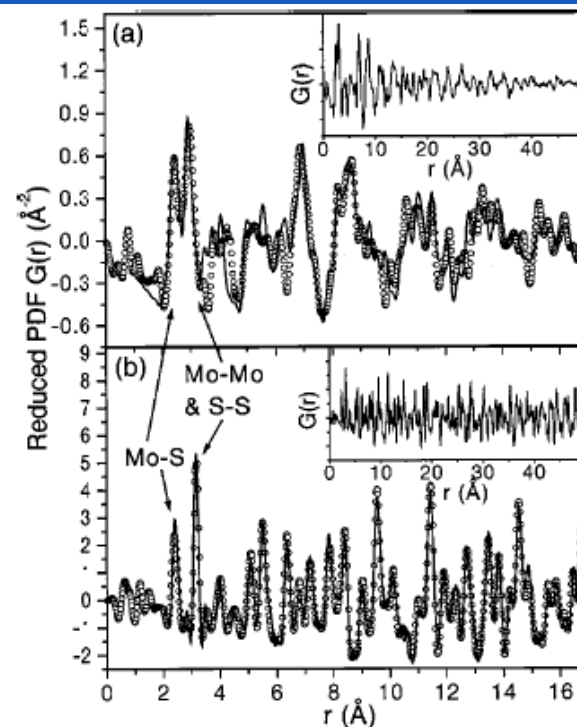
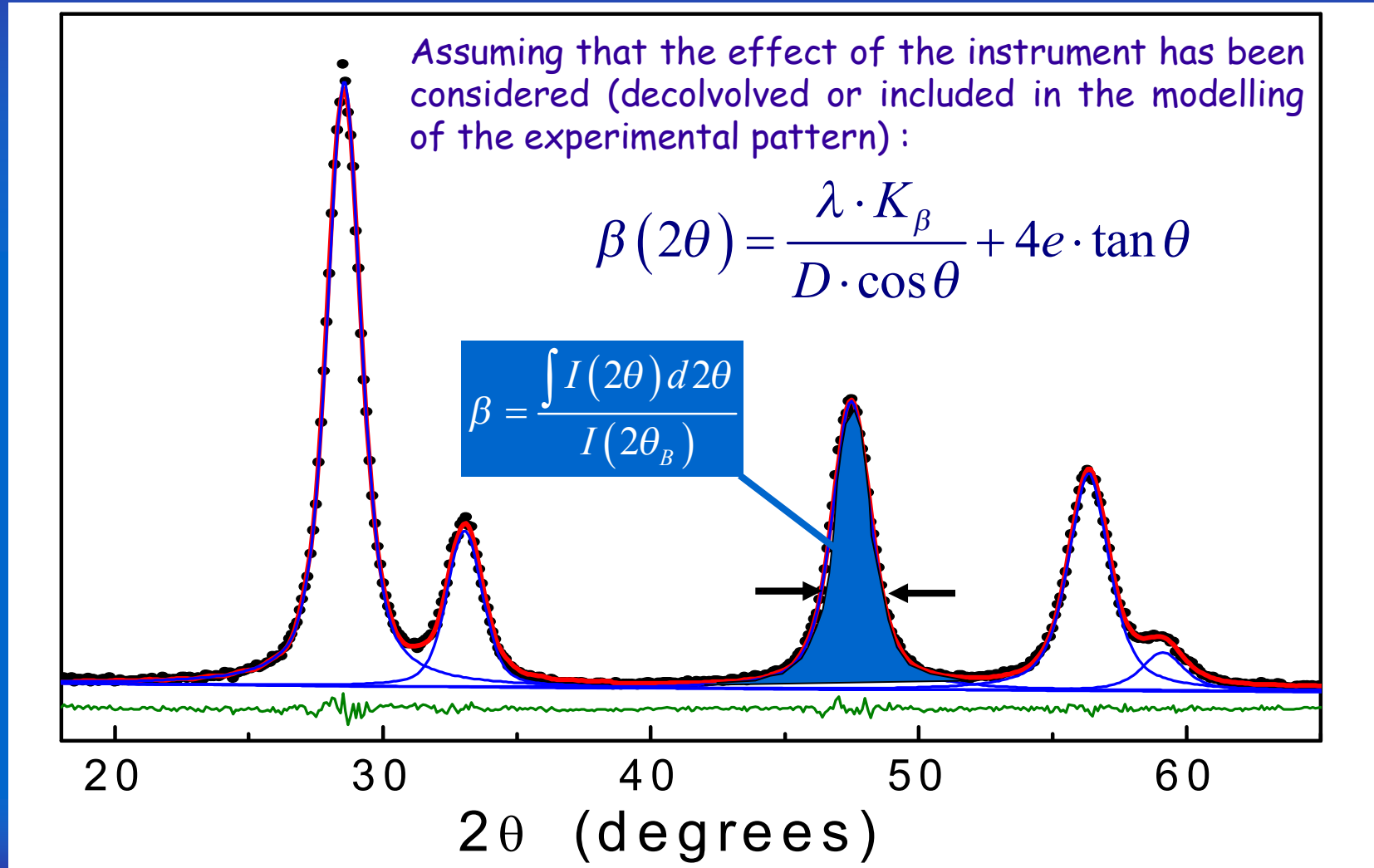


FIG. 2. Experimental (dots) and fitted (solid line) PDF's for  $\text{LiMoS}_2$  (a) and  $\text{MoS}_2$  (b). Note the different scale between (a) and (b). The first two peaks in the PDF's are labeled with the corresponding atomic pairs. The experimental data are shown in an expanded scale in the insets.



# LINE PROFILE ANALYSIS

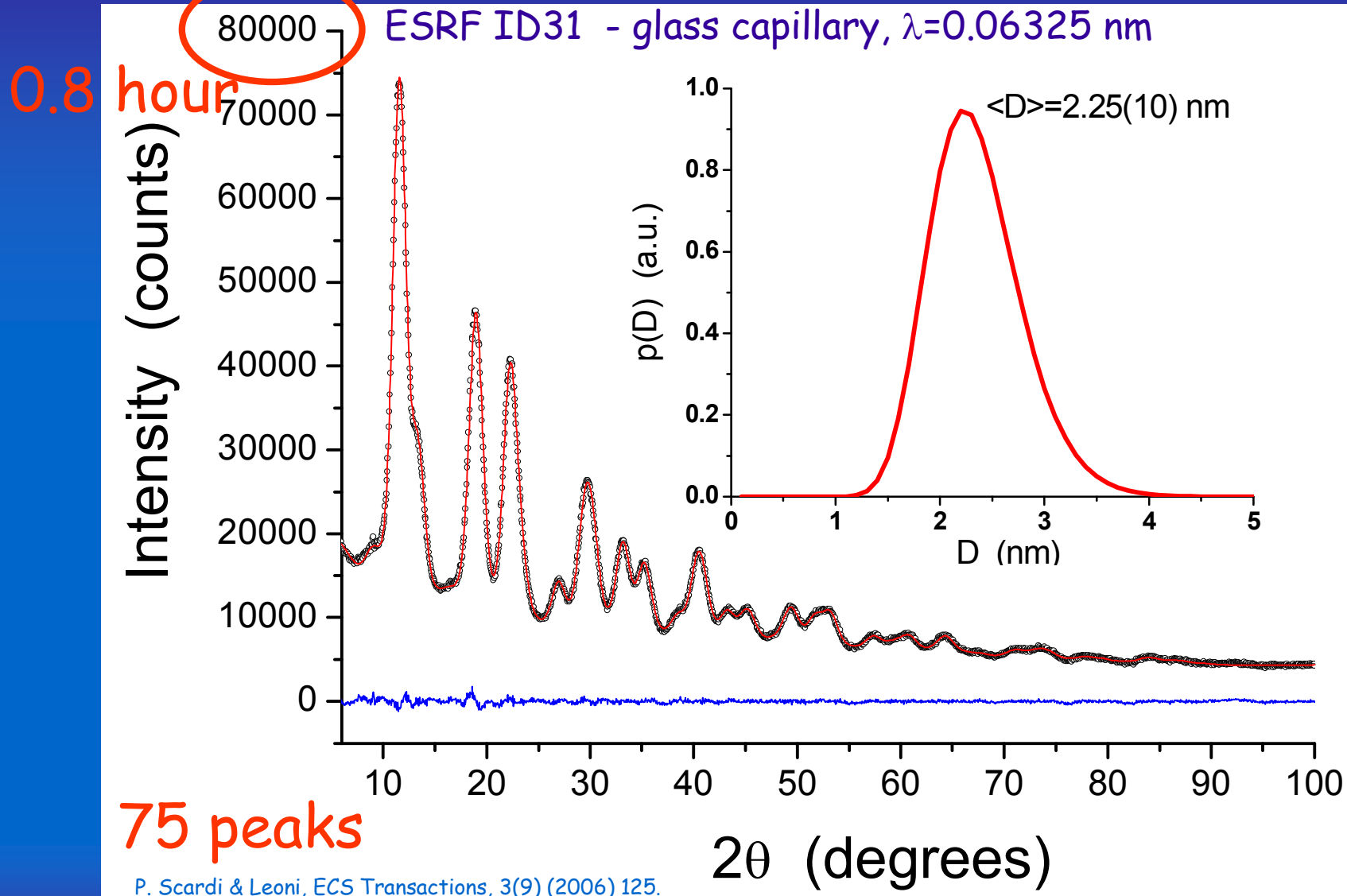
By taking the integral breadth  $\beta(2\theta)$  (ratio between peak area and maximum) as a measure of the peak profile width (shape):





# LINE PROFILE ANALYSIS: SRXRD

Xerogel obtained by vacuum-drying: broad diffraction lines of nanocrystalline fcc phase

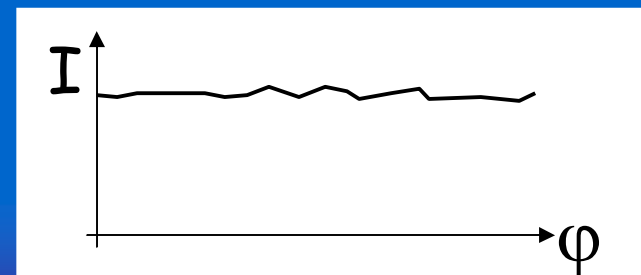
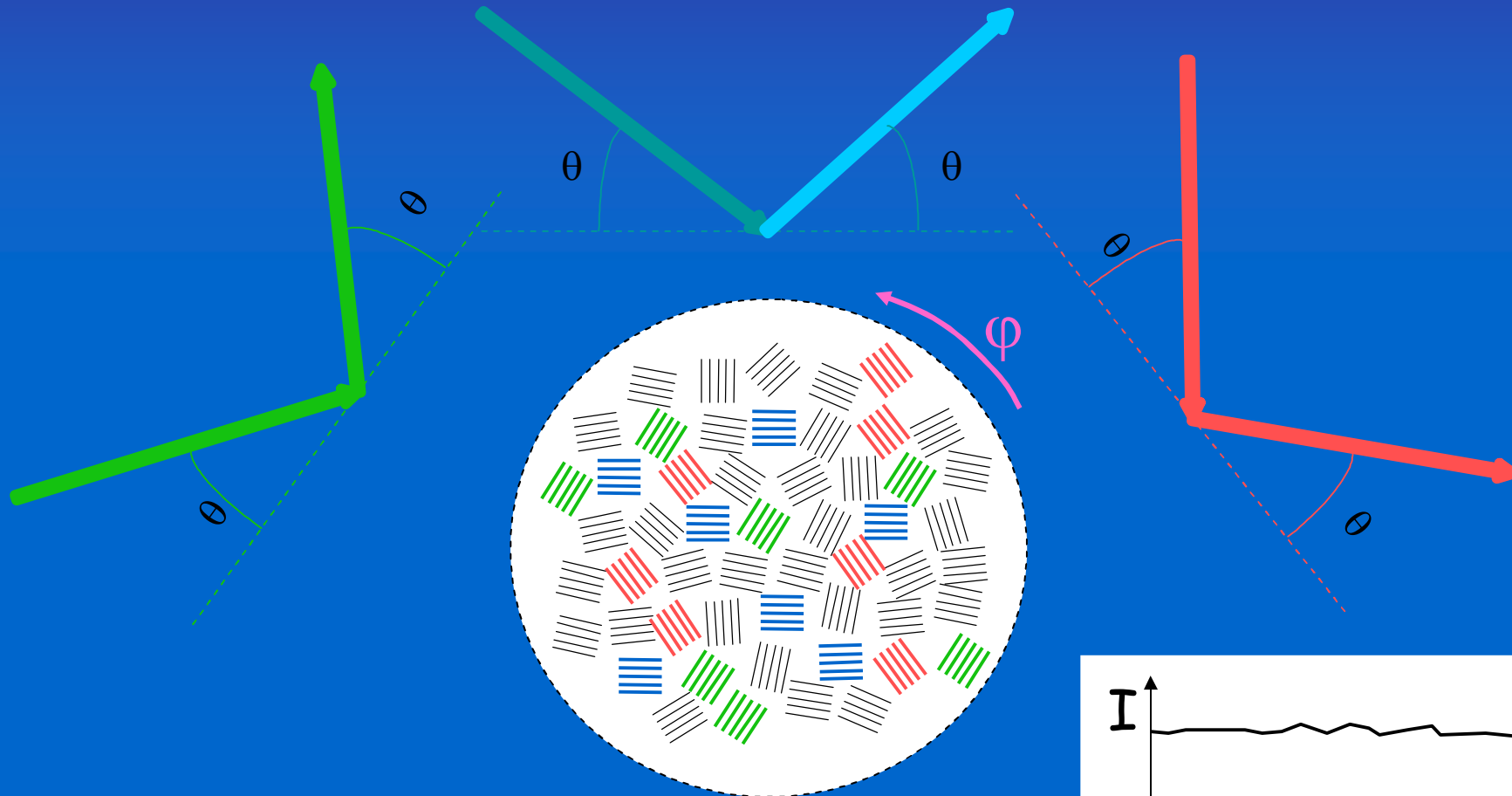


P. Scardi & Leoni, ECS Transactions, 3(9) (2006) 125.



# TEXTURE ANALYSIS

A 'true' powder has randomly oriented crystalline domains.  
The diffracted intensity does not depend on the probing direction.



for any  $hkl$

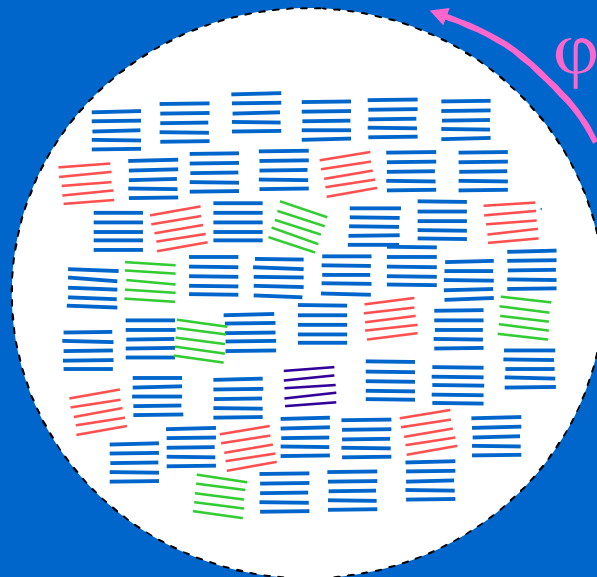
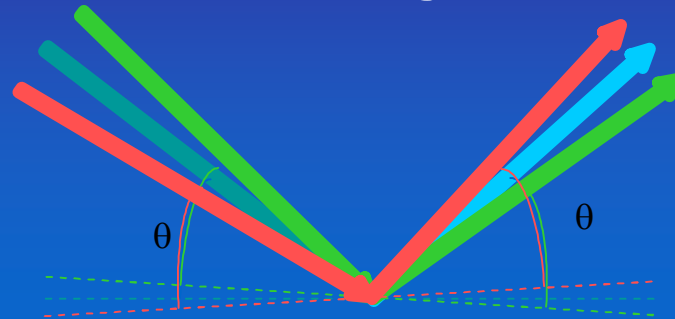
random orientation



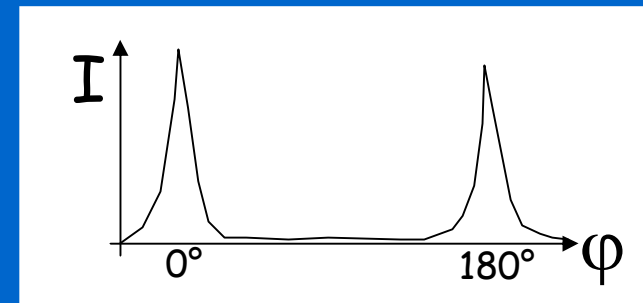


# TEXTURE ANALYSIS

If the grain (crystal) orientation is not random, the diffracted signal depends on the incident angle.



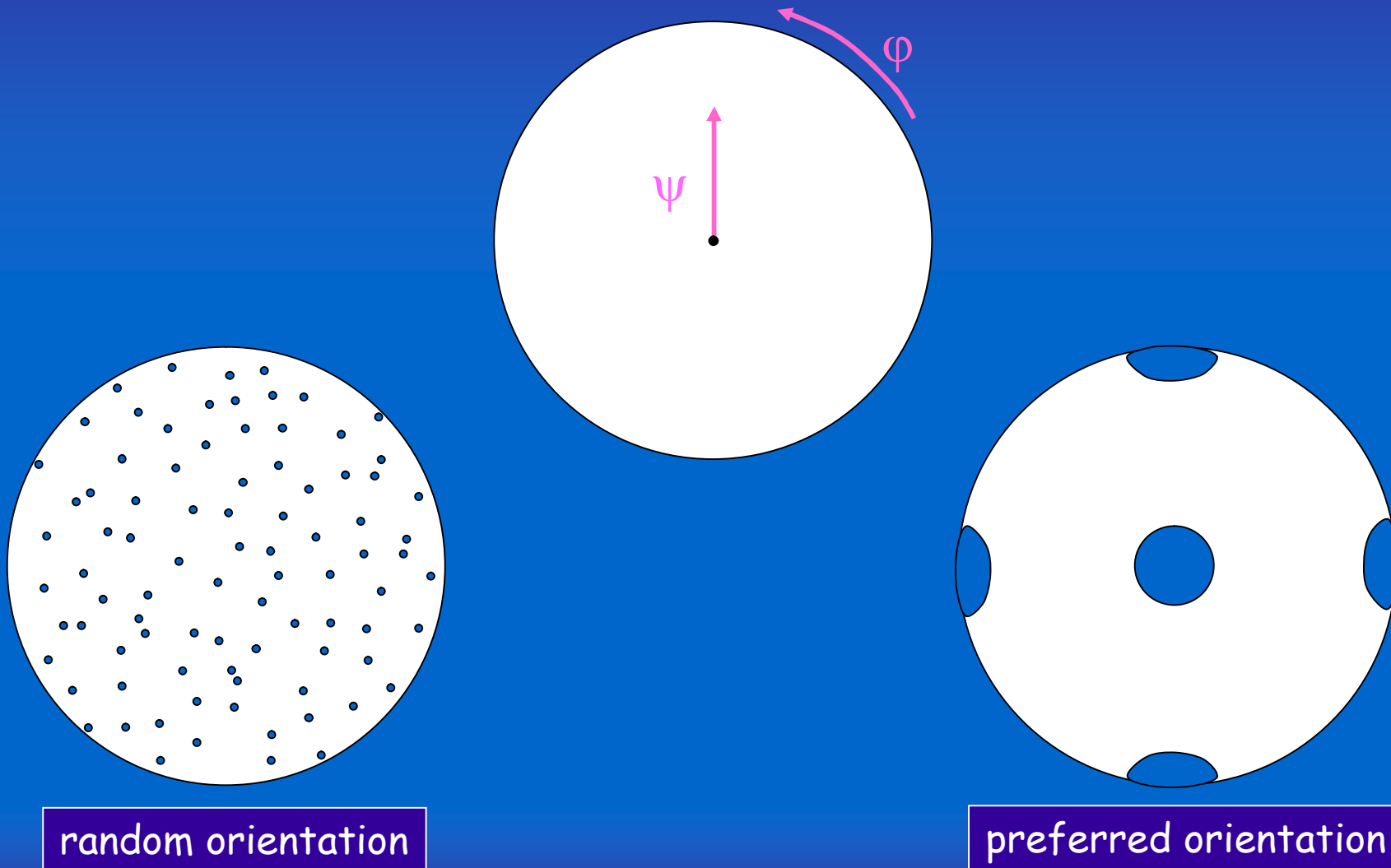
preferred orientation





# TEXTURE ANALYSIS

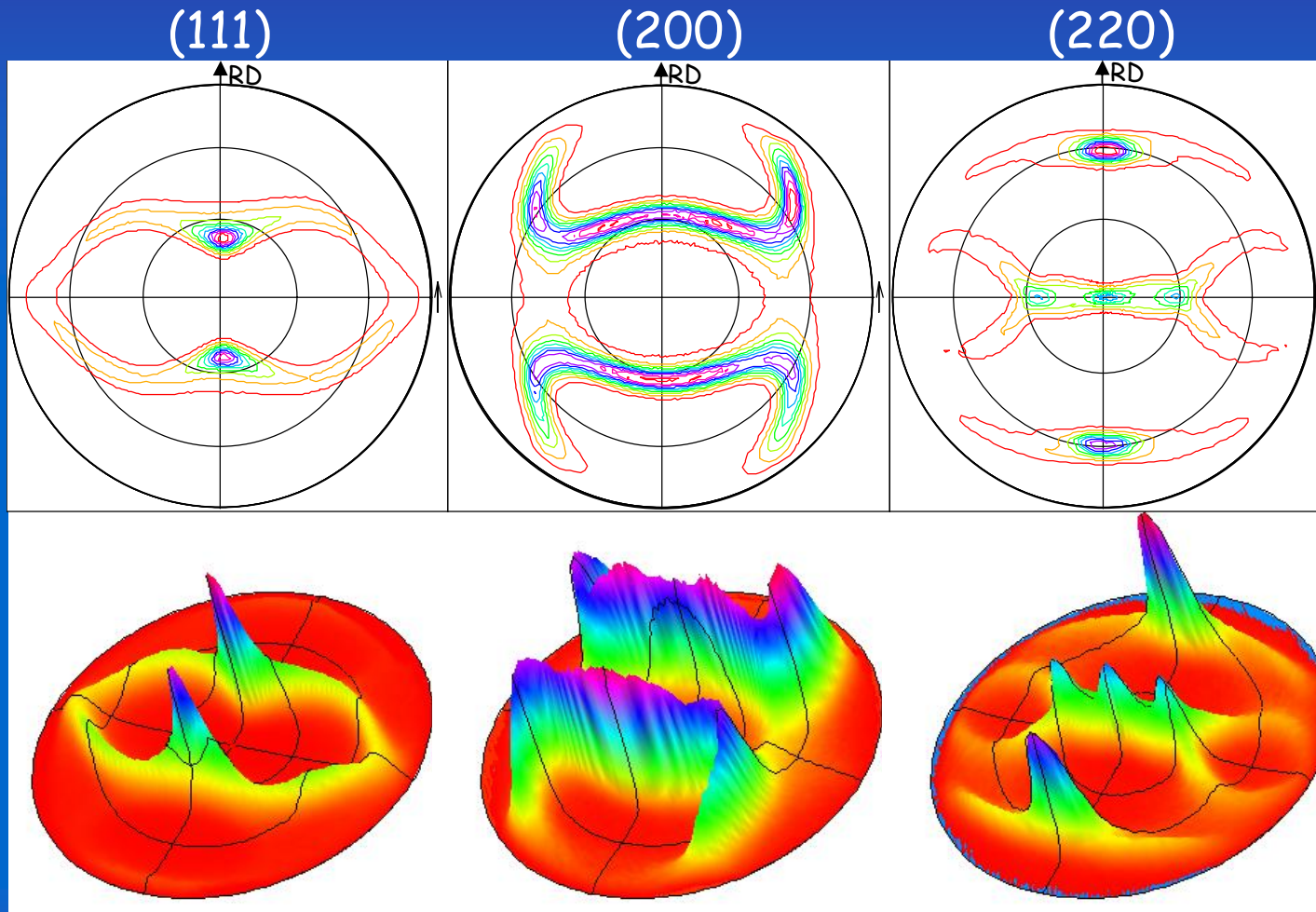
Crystallographic texture: pole figures





# TEXTURE ANALYSIS

In general, texture can be quite complex. Several pole figures, for different (hkl), may be required to understand the orientation

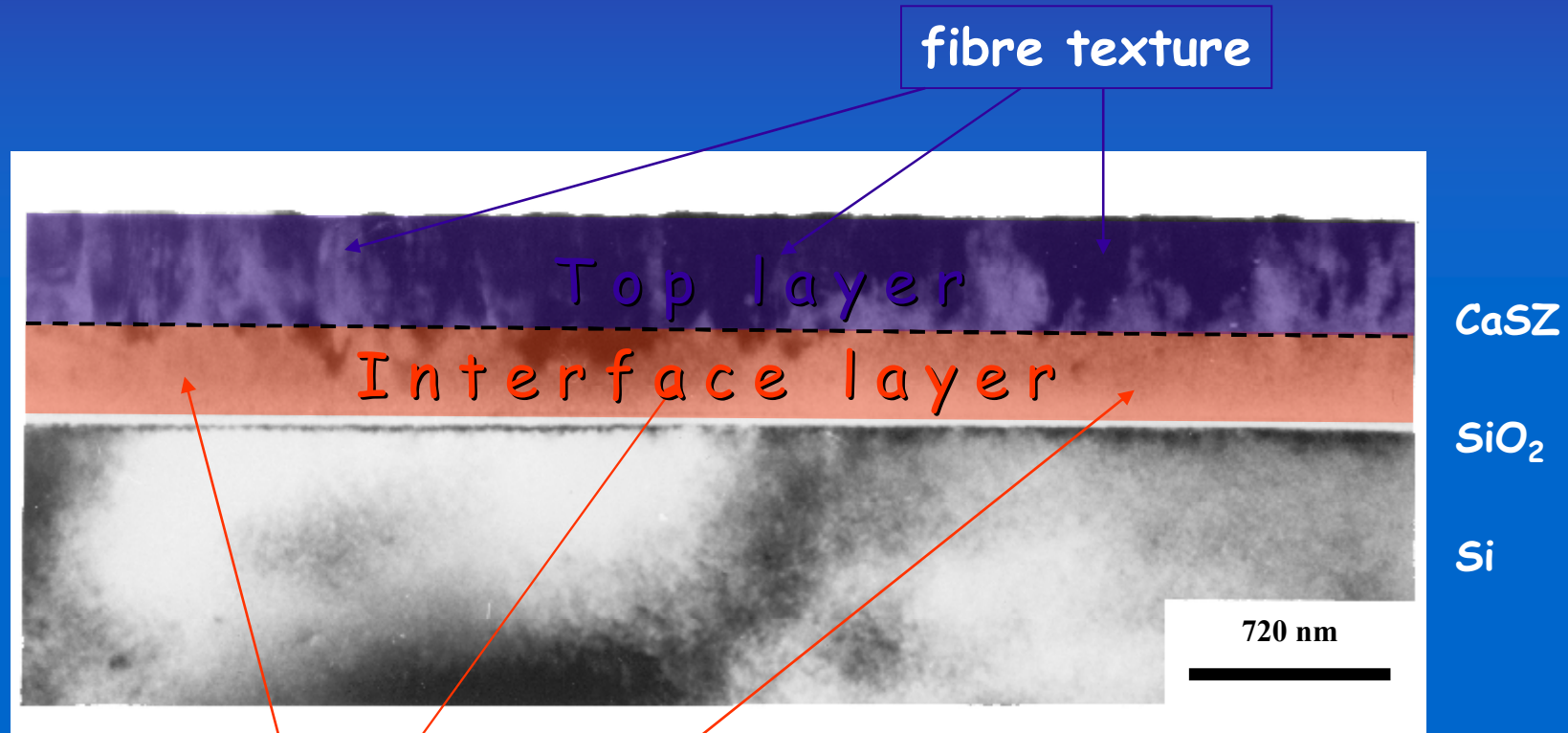


Cold-rolled Ni for high- $T_c$  superconducting wires



# TEXTURE GRADIENT BY SRXRD

In absence of epitaxy, PVD thin films tend to be polycrystalline at the interface and develop a fibre texture with increasing thickness

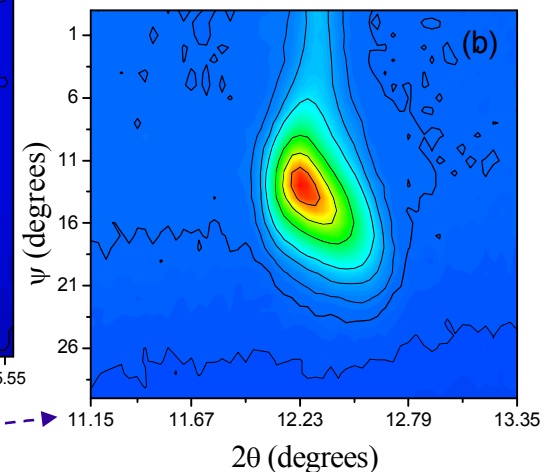
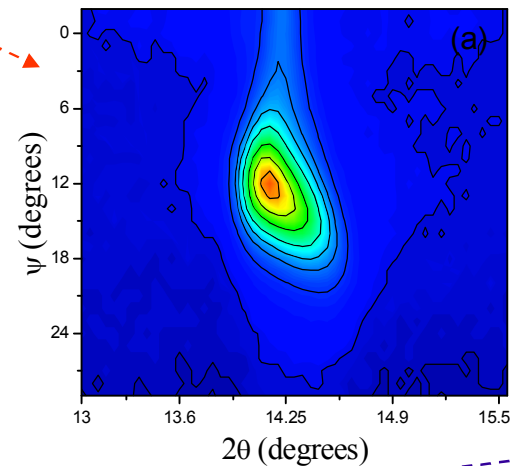
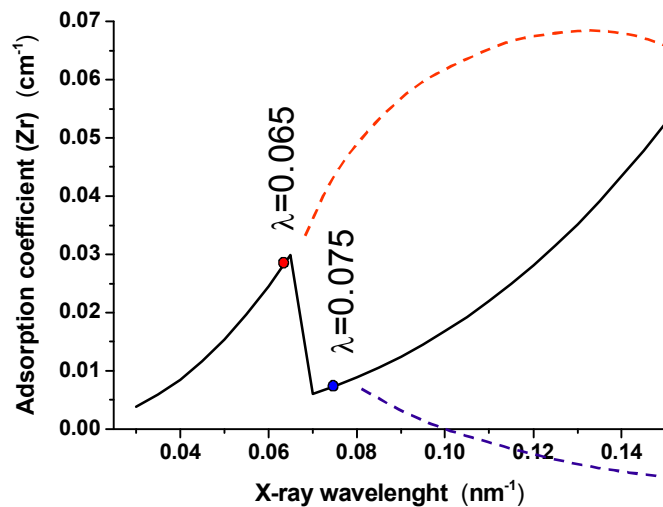
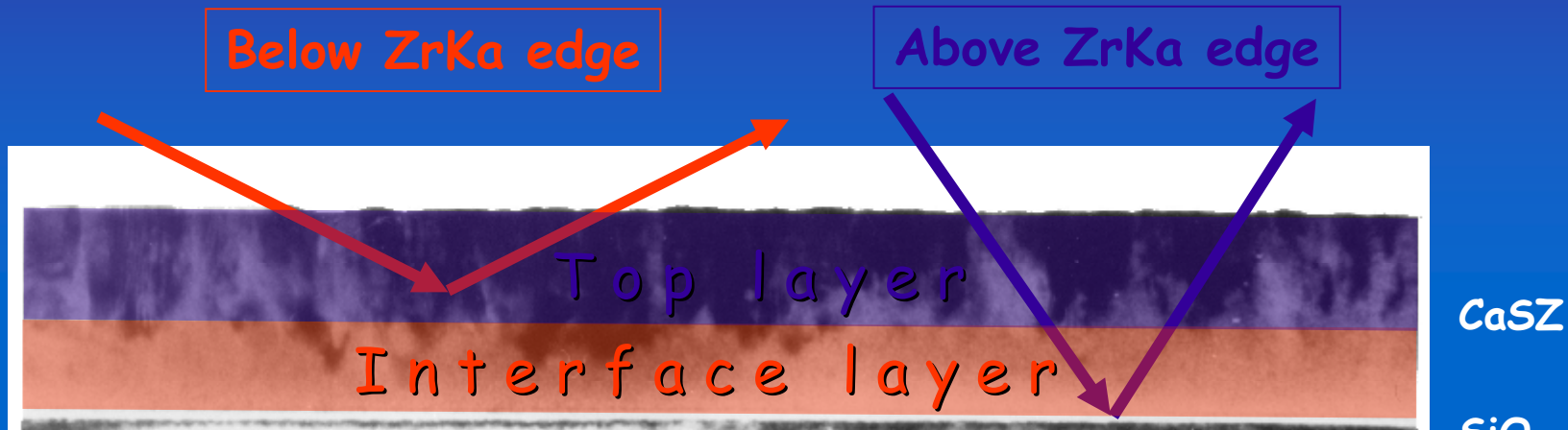


polycrystalline (random oriented grains)



# TEXTURE GRADIENT BY SRXRD

Using X-rays with energy just below and just above the adsorption edge of Zr, different contributions are obtained from the two layers



P. Scardi, Leoni, M. D'Incau, Thin Solid Films, 467 (2004) 326.



# RESIDUAL STRESS ANALYSIS

Crystalline domains can be used as strain gauges

grain deformation

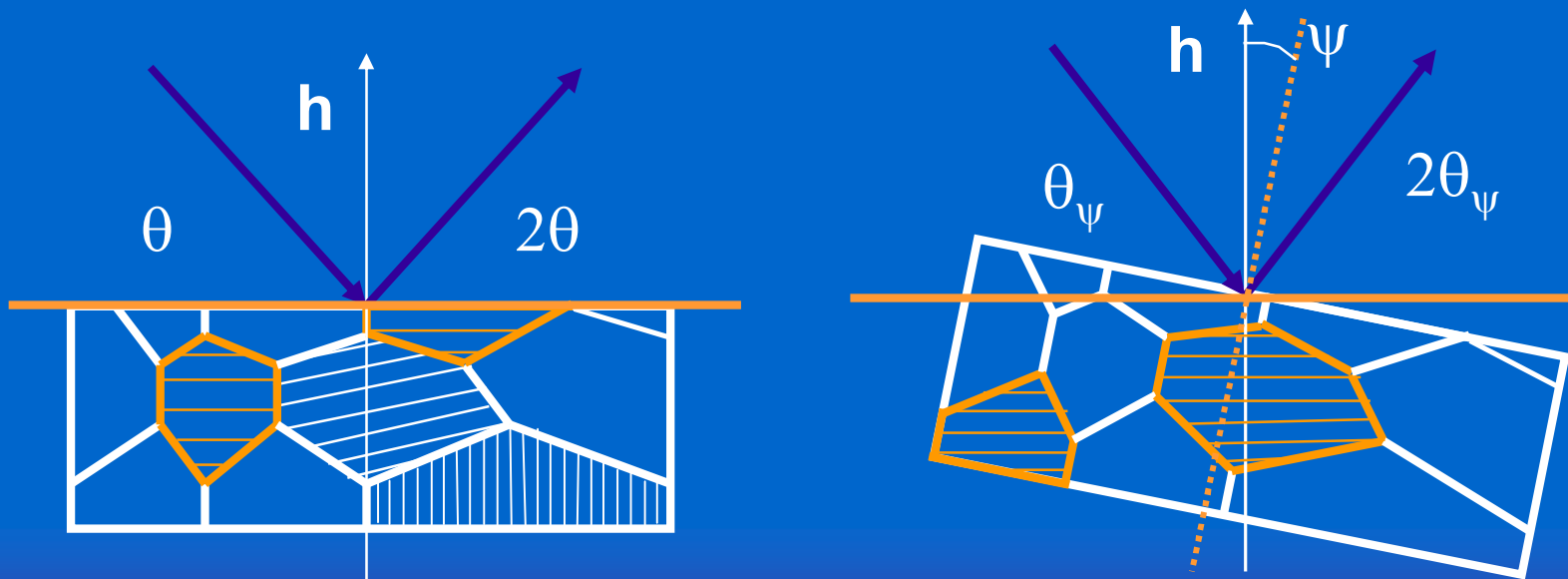
$$\varepsilon = \frac{\Delta l}{l}$$



lattice deformation

$$\varepsilon = \frac{\Delta d}{d}$$

The deformation is measured along different directions, by tilting the sample. The in-plane strain is obtained by measuring  $d$  along off-plane directions.





# RESIDUAL STRESS ANALYSIS

If the stress field is plane and rotationally symmetric:

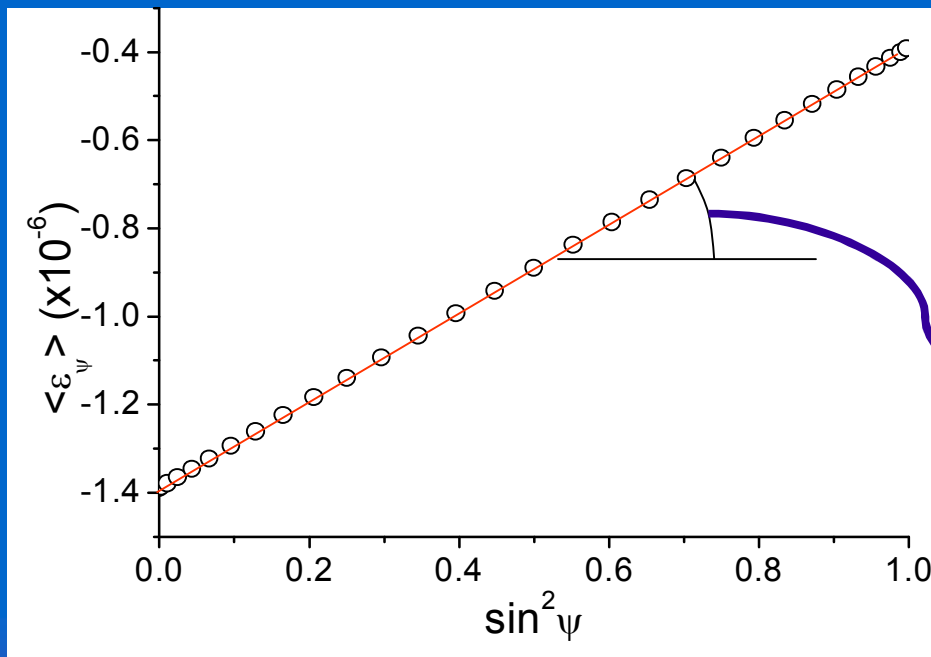
$$\sigma_{11} = \sigma_{22} = \sigma_{\parallel}, \quad \sigma_{12} = \sigma_{13} = \sigma_{23} = \sigma_{33} = 0$$



and if no gradient and no texture are present, then:

$$\langle \varepsilon_{\psi}^{hkl} \rangle = \left( 2S_1^{hkl} + \frac{1}{2}S_2^{hkl} \sin^2 \psi \right) \sigma_{\psi}^S$$

"sin<sup>2</sup>ψ formula"



$$S_1^{hkl}, \quad \frac{1}{2}S_2^{hkl}$$

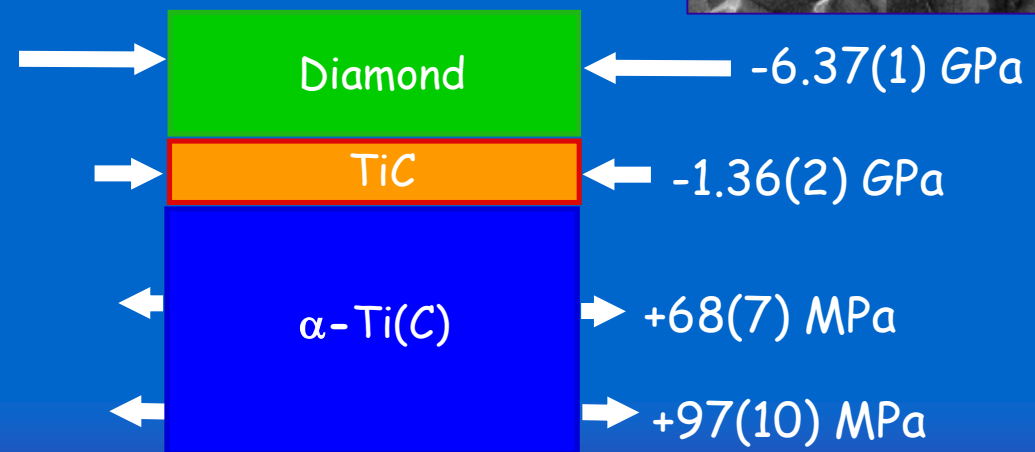
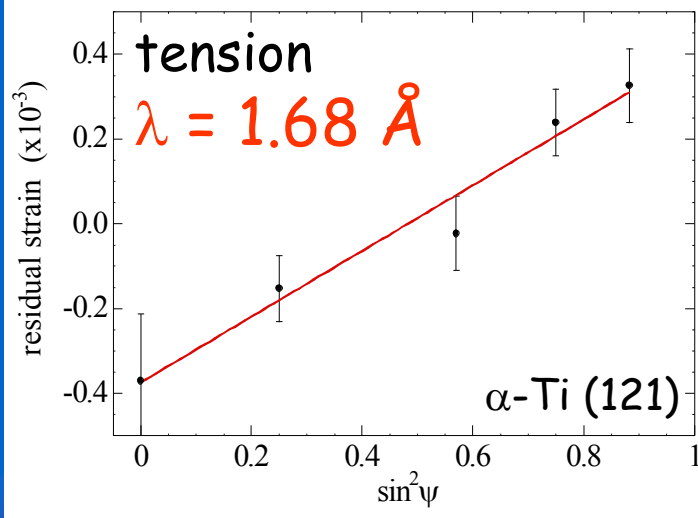
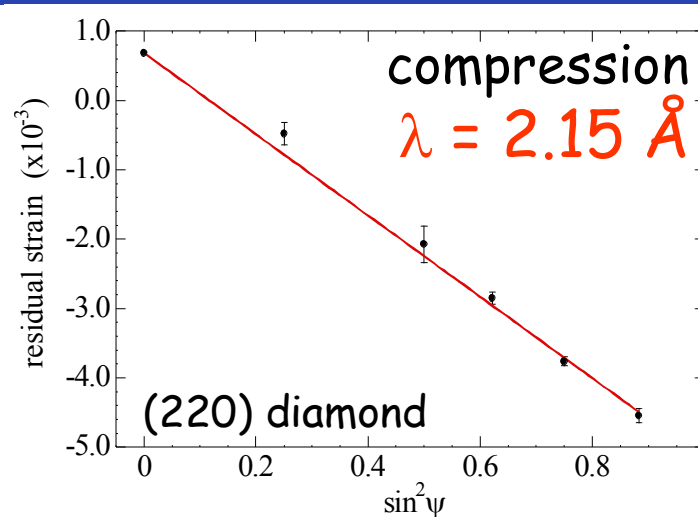
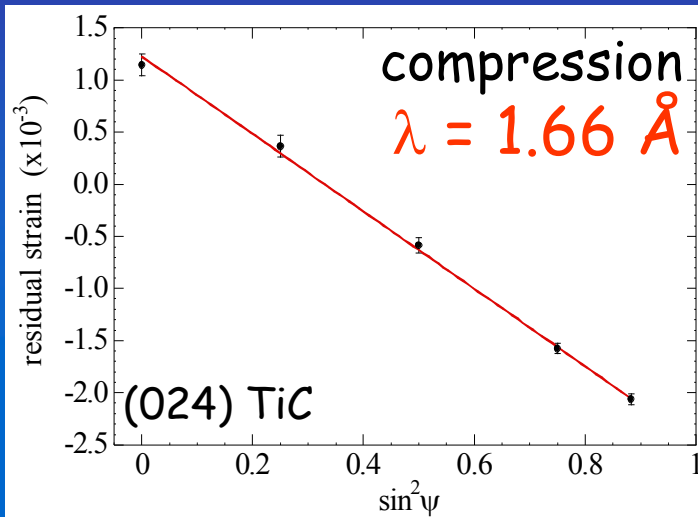
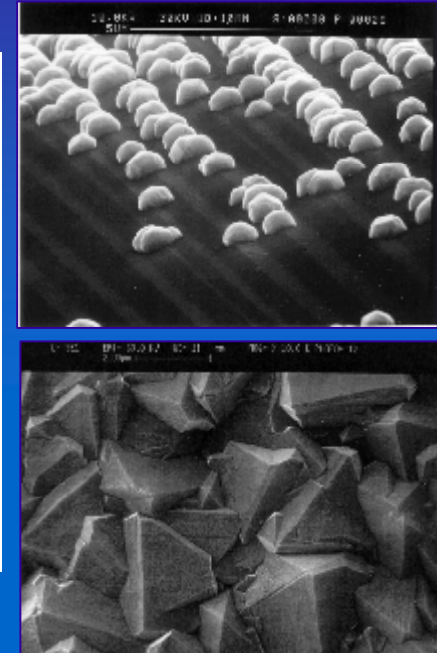
X-ray elastic constants (XECs)

slope related to the average in-plane stress



# RESIDUAL STRESS GRADIENT BY SRXRD

Residual stress in diamond coated components: multiple wavelength XRD

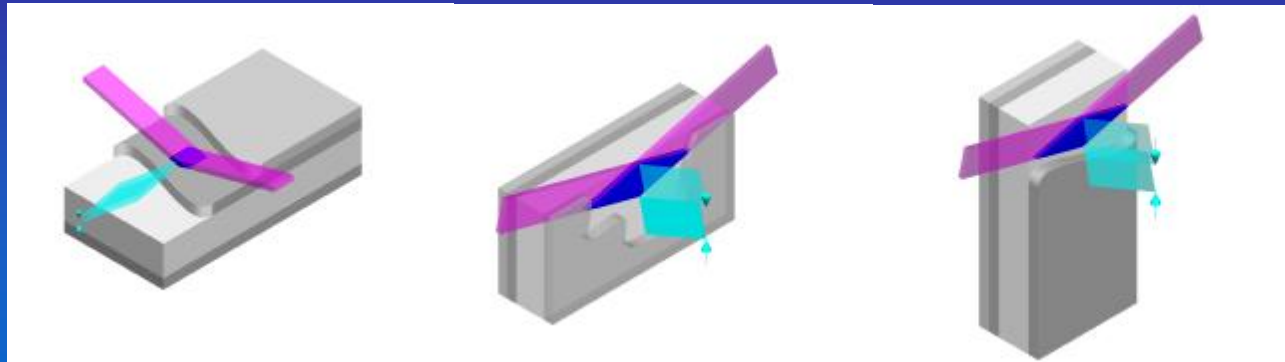




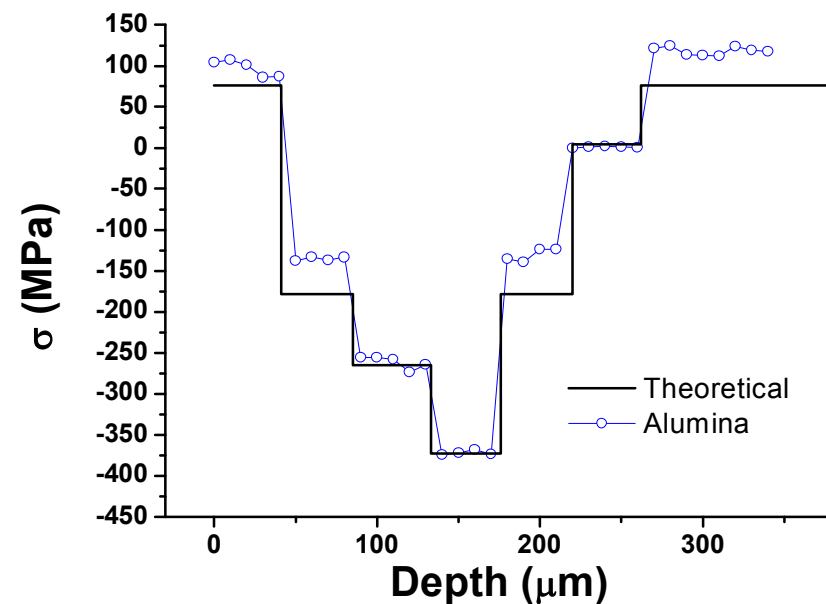
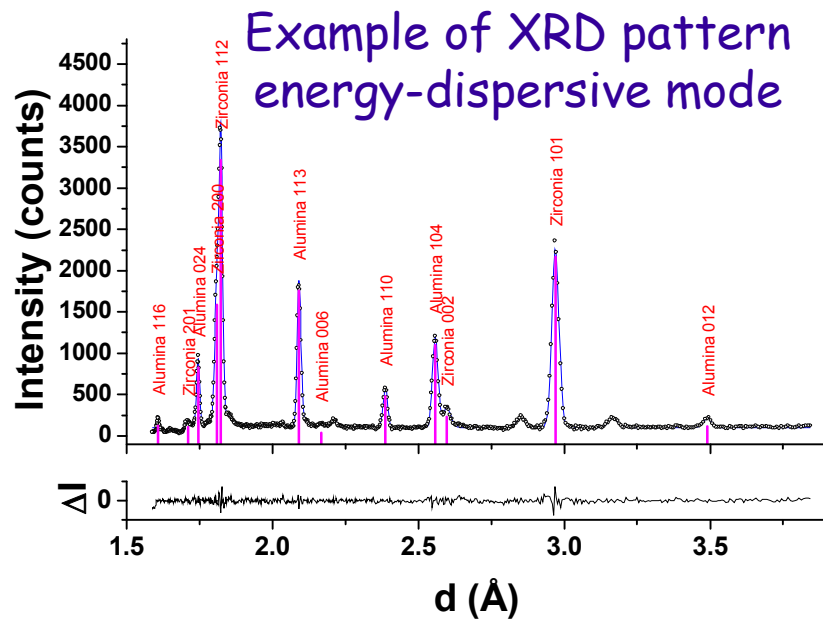


# RESIDUAL STRESS GRADIENT BY SRXRD

Possible geometries for through-thickness stress mapping

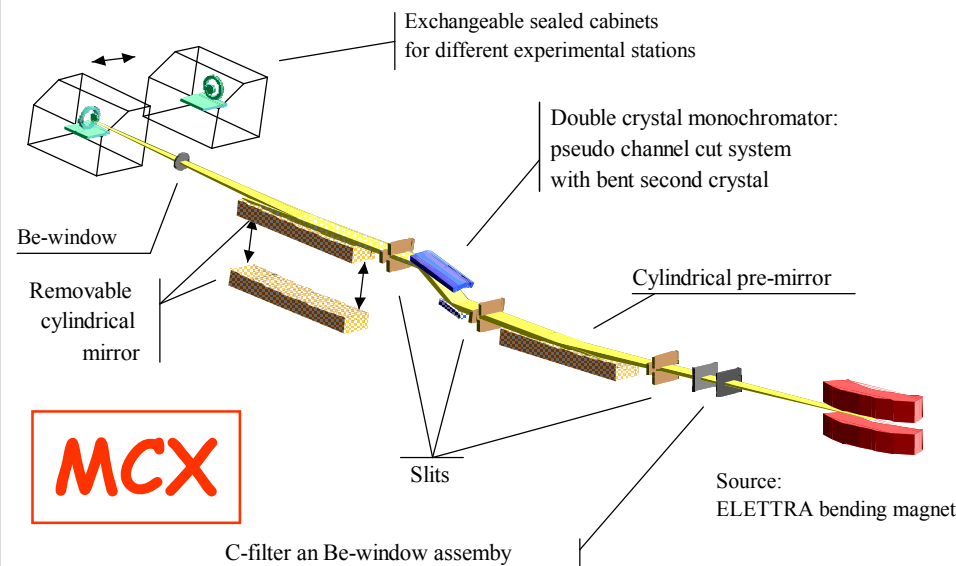


Residual stress profile in a Alumina-Zirconia-Mullite ceramic laminates





**MCX - A new beamline for Materials Characterization by XRD at ELETTRA (Trieste, Italy)**  
G. Paolucci, E. Busetto, A. Lausi, J. Plasier (Sincrotrone Trieste), P. Scardi (Univ. Trento & INSTM)



## Examples of typical applications

- Residual stress and texture analysis in thin films by multiple wavelength XRD
- Surface analysis by grazing incidence XRD and reflectivity
- Medium-low energy (3.5÷20 keV) anomalous scattering XRD
- Line Profile Analysis (e.g., nanocrystalline, highly defected materials)
- Non-ambient studies (controlled atmosphere, high temperature kinetics)
- Surface mapping by microdiffraction (diffraction on small area)



# REFERENCES

- [1] B.D. Cullity, *Elements of X-ray Diffraction*, Addison-Wesley, Reading MA, 1978.
- [2] R. Jenkins & R. L. Snyder, *Introduction to X-ray Powder Diffractometry*, Wiley, New York, 1996
- [3] H.P. Klug & L.E. Alexander, *X-ray Diffraction procedures*, Wiley, New York, 1974.
- [4] B.E. Warren, *X-ray Diffraction*, Addison-Wesley, Reading, MA, 1969.
- [5] R.A. Young, *The Rietveld method*, Oxford University Press, Oxford, 1993.
- [6] International Tables for X-ray Crystallography, 3<sup>rd</sup> series. [Kluwer Academic Publishers](http://www.kluweronline.com/), Dordrecht, Boston, London. Vol.A (1983), Vol.B (1993), Vol.C (1992), "Brief Teaching Edition of Volume A" (1985).
- [7] P.P. Ewald, *Fifty years of X-ray Diffraction*, Reprinted in pdf format for the IUCr XVIII Congress, Glasgow, Scotland. Copyright © 1962, 1999 International Union of Crystallography, Chester, UK.
- [8] International Union of Crystallography: <http://www.iucr.org>
- [9] International Centre for Diffraction Data, Newtown Square, PA, USA. <http://www.icdd.com>
- [10] CCP14 : <http://www.ccp14.ac.uk/> ; <http://www.iucr.org/sincriis-top/logiciel/index.html>

Paolo.Scardi@unitn.it